Journal of Mammalian Evolution (2026) 33:26
https://doi.org/10.1007/s10914-026-09819-1

RESEARCH

The influence of ecology and phylogeny on the canid frontal sinus

Samuele Frosali[1] · Alessandro Urciuoli[2,3,4,5] · Joan Madurell-Malapeira[6] · Lorenzo Rook[6] · Saverio Bartolini-Lucenti[3,6]

Received: 25 August 2025 / Accepted: 6 April 2026
© The Author(s) 2026

Abstract

Despite the fact that a well-developed frontal sinus is an apomorphy evolved only in the subfamily Caninae, important ecological factors might have played a role in the development of this paranasal cavity. Here, we present the first analysis of the 3D morphology of three fossil species of the genus *Canis* using an innovative deformation-based morphometric approach. Our aim was to disentangle the relative contributions of phylogenetic relationships and ecological adaptations. Based on the reconstructed morphology of the fossil species sinuses, we were able to corroborate and to better reconstruct the palaeodiet of the analysed fossil taxa. In particular, the overall structure and morphology of the frontal sinus of *Canis etruscus* suggests a lower proportion of meat in its diet. This species also displays the most primitive morphology among the three fossil species analysed, indicating an ancestral condition within the Canina lineage. On the other hand, the sinus shape and size of *Canis mosbachensis* and *Canis borjgali* suggest a higher proportion of meat consumption. In particular, *C. borjgali* closely resembles the extant wolf (*Canis lupus*) condition and suggests a possible hypercarnivorous group-hunting adaptation. Our results thus indicate that ecology is the primary driver of frontal sinuses shape and size, whereas phylogeny accounts for differences at higher taxonomic levels (i.e., subtribe level), highlighting how the analysis of this paranasal cavity can help in the further comprehension of both the paleoecology and phylogeny of fossil canids.

Keywords Canid · Diet · Frontal sinus · Palaeoecology · Phylogeny

Introduction

The subfamily Caninae Fischer von Waldheim, 1817 represents the only living group of the family Canidae Fischer von Waldheim, 1817 (Tedford et al. 2009). During the Late Miocene, they experienced an initial adaptive radiation linked to the evolution of a more hypocarnivorous diet, which led to the diversification of numerous fox-like species (Wang et al. 2008). Following the Late Miocene, the subfamily underwent a second diet-driven adaptive radiation linked to the expansion of the nasal cavity into the frontal bone (Wang et al. 2008). The evolutionary history of the subfamily gave rise to two tribes that are distinguished based on this feature, the Vulpini Hemprich and Ehrenberg, 1830 (they do not possess this feature) and the Canini Fischer von Waldheim, 1817 (they do possess an inflated frontal bone). Both tribes underwent a process of adaptive radiation, firstly the tribe Vulpini, whose representative were among the first species of the Caninae to colonize the Old World between the Late Miocene and Early Pliocene (Tedford and Wang 2008). Within the Canini tribe, the adaptive radiation began instead in

✉ Samuele Frosali
samuele.frosali@unifi.it

1 Museo di Geologia e Paleontologia, Università di Firenze, Via La Pira 4, Florence 50121, Italy

2 Department of Paleontology, University of Zurich, Karl-Schmid-Strasse 4, Zurich 8006, Switzerland

3 Institut Català de Paleontologia Miquel Crusafont (ICP-CERCA), Universitat Autònoma de Barcelona, Edifici ICTA-ICP, c/ Columnes s/n, Campus de la UAB, Cerdanyola del Vallès, Barcelona 08193, Spain

4 Division of Paleoanthropology, Senckenberg Research Institute and Natural History Museum Frankfurt, Senckenberganlage 25, Frankfurt am Main 60325, Germany

5 Departemento de Ciencias de la Vida, Universidad de Alcalá, Cátedra de Otoacústica Evolutiva y Paleoantropología (HM Hospitales-UAH), Alcalá de Henares, Madrid 28871, Spain

6 Dipartimento di Scienze della Terra, Università degli Studi di Firenze, Via La Pira 4, Florence 50121, Italy

Published online: 22 May 2026

North America with the genus *Eucyon* Tedford and Qiu, 1996 during the latest Miocene (Bartolini-Lucenti and Rook 2021). This genus was one of the first canid colonizers of Eurasia and Africa, where it thrived and diversified, becoming an important element of Eurasian and African Pliocene faunas (Bartolini-Lucenti and Rook 2021). The diversification of *Eucyon* in the latest Miocene of Eurasia and Africa corresponds to one of the two main adaptive radiations in the history of Caninae that Sotnikova and Rook (2010) defined as the "*Eucyon* event". The other main event of diversification took place during the Late Pliocene, when the genus *Canis* radiated, and was thus termed as the "*Canis* event" (Sotnikova and Rook 2010). This event caused a species turnover in the faunas of the Old World during which the species of the genus *Eucyon* went almost completely extinct. These were soon thereafter replaced by many species of the genus *Canis* sensu lato (e.g., *Canis teilhardi* Qiu et al., 2004, *Canis longdanensis* Qiu et al., 2004, *Canis (Xenocyon) brevicephalus* Qiu et al., 2004, *Canis (Xenocyon) dubius* (Teilhard de Chardin, 1940), *Canis etruscus* Forsyth Major, 1877, *Canis arnensis* Del Campana, 1913, *Canis borjgali* Bartolini-Lucenti et al., 2020, *Canis (Xenocyon) falconeri* Forsyth Major, 1877; see Sotnikova & Rook 2010).

Frontal sinus in canids: status quo

The frontal sinus represents an expansion of the nasal cavity into the frontal bone: the two cavities are connected through the nasofrontal opening (apertura sinus frontalis; Evans et al. 2013). The presence/absence of this feature is often used as the main trait distinguishing the two tribes of the subfamily Caninae (Wang et al. 2008). In particular, the Vulpini show the primitive condition shared by almost all the living true foxes belonging to the genus *Vulpes* Frisch, 1775. This is represented on the outer surface of the skull by a shallow depression on the dorsal surface of the postorbital process called "vulpine crease" (this condition is due to the lack of a developed frontal sinus). Conversely, the Canini show the derived morphology, with an inflated frontal bone that derives from the expansion of the nasal cavity in the frontal bone creating the frontal sinus (Tedford et al. 1995).

The first author to use the frontal sinus as a feature for distinguishing among the two tribes was Huxley (1880). Even though this character was initially strongly criticised by the scientific community, it is now widely accepted. In recent years, the study of paranasal cavities acquired more and more interest in paleontology and paleoantrhopology for its potential in phylogenetic, biomechanical and ecological analyses (e.g., Balzeau et al. 2022; Iurino et al. 2022; Frosali et al. 2023).

As stated above, in canids, the frontal sinus represents a synapomorphy of the tribe Canini, with the most distinct condition found in the genus *Canis* Linnaeus, 1758, where the sinus reaches the frontoparietal suture. In *Canis*, the frontal sinus is responsible for the convex morphology of the dorsal surface of the cranium above the orbits, as well as of a widening of the postorbital constriction (Frosali et al. 2023).

Based on the evidence derived from other carnivoran families (e.g., Hyaenidae Gray, 1821), the most commonly accepted hypothesis for the development of a frontal sinus in canids posits a role of this structure in the dissipation of feeding stresses. Some studies (e.g., Curtis and Van Valkenburgh 2014) have also highlighted a correlation between the shape and size of this structure and diet (the softer the food eaten, the smaller the frontal sinus). Frosali et al. (2023), who first thoroughly investigated the frontal sinus morphology in fossil canids, reaffirmed this hypothesis and suggested that this paranasal cavity represents an important tool for reconstructing the paleoecology in fossil canids. The link between morphology and size of the frontal sinus, and its role in the dispersal of feeding stresses have also been confirmed by Peri et al. (2025), who investigated the stress dispersion patterns in a few extant and extinct canid species. However, the function of the frontal sinus is not entirely clarified and probably other ecological factors (e.g., brain thermoregulation, olfactory enhancement abilities, etc.) might be involved in shaping the morphology of this paranasal cavity (Joeckel 1998; McGreevy et al. 2004; Vinuesa et al. 2015). These other ecologically oriented hypotheses are based on the assumed link between the frontal sinus and the respiratory system. This cavity indeed forms from the breaking down of the cartilage that composes the developing nasal capsule, which allows the vascular, osteoclastic lamina propria and the nasal epithelium to protrude outside the nasal chamber and invade the bones surrounding the nasal chamber (Curtis and Van Valkenburgh 2014).

Our study aims to investigate the morphological variation of the frontal sinus in fossil canids, in particular of the genus *Canis*, to better assess its palaeoecological implications, especially in relation to the feeding stresses associated with dietary adaptations. We expect a direct correlation between the feeding stresses and strains and the size of the frontal sinus. Our study represents the first attempt to characterise the sinus morphology of three fossil species of the genus *Canis* and tries to discriminate among the influences of ecology and phylogeny on frontal sinus morphological variation.

Materials and methods

Comparative and studied material

The dataset used in this study represents an expansion of that of Frosali et al. (2023) thanks to the addition of comparative material belonging to species of the subtribe Cerdocyonina

Tedford et al., 2009 (the so-called South American canids) and the only species of the tribe Vulpini that possesses a frontal sinus, *Nyctereutes procyonoides* (Gray, 1834). This addition was aimed to better assess the variation of the Caninae as a whole, and not just the subtribe Canina Fischer von Waldheim, 1817. The extant comparative sample includes: *Atelocynus microtis* (Sclater, 1883): MZUF-1518; *Canis aureus* (Linnaeus, 1758): CBL 153, CBL 296, CBL 297, CBL 298, CBL 299, MZUF-11878, MZUF-11880, 016_C_GDJK, 016_C2_GDJK, 016_C3_GDJK; *Canis latrans* Say, 1823: RD_0008, UCLA 1225, UCLA SO 2739, 038_C_COY, UAMC 88-50-290; *Canis lupaster* Hemprich and Ehrenberg, 1833: MZUF-1851, MZUF-2110, MZUF-2140, MZUF-2714; *Canis lupus* Linnaeus, 1758: AMNH 99667, AMNH 99679, AMNH 132868, CBL 117, DST-N01, MZUF-2032, MZUF-11874, MZUF-16534; *Canis simensis* Rüppell, 1835: AMNH m-81001, CE818, MZUF-13781; *Cerdocyon thous* Linnaeus, 1766: MZUF-4062; *Chrysocyon brachyurus* Illiger, 1811: MAM017321, 147_C _MAWO; *Lupulella adusta* (Sundevall, 1846): MZUF-8496, TM1942, TM8684; *Lupulella mesomelas* (Schreber, 1775): MZUF-1128, MZUF-1715, MZUF-1843, MZUF-1898, MZUF-3293, TM1571, TM3028, UCLA 3000; *Lycaon pictus* (Temminck, 1820): AZ11895, AZTM2244, CBL 978, MZUF-1127, TM5560, TM47678, USNM 368441, USNM 368443; *Nyctereutes procyonoides*: BLOC 210119, USNM 255530; *Vulpes lagopus* (Linnaeus, 1758): MZUF-1474.

The studied material benefited also from the inclusion of four extinct species of the genus *Canis*: one cranium of *C. arnensis* stored at the Geology and Paleontology Museum of Florence (IGF 869), one cranium of *Canis mosbachensis* Soergel, 1925 currently stored at the Institut Mediterrani d'Estudis Avançats (IMEDEA-C2), two crania of *C. etruscus* currently stored at the Geology and Paleontology Museum of Florence (IGF 4407, IGF 4412) and a specimen of *C. borjgali* stored at the S. Janashian Museum of Georgia, Georgian National Museum, in Tbilisi (D64).

Data acquisition

To perform quantitative and qualitative analysis of the frontal sinus we relied on computed tomography (CT) and microcomputed tomography (μCT) digital images. All the scanning information for each specimen has been reported in Online Resource 1: Table S1 (while the information on the Institutional abbreviations are all reported in Online Resource 1: Table S2). The slice stacks obtained from the CTs and μCTs were imported into 3D Slicer software (ver. 5.6.2, www.slicer.org; Fedorov et al. 2012) to perform manual segmentation and digitally extract the 3D models of the frontal sinuses. To perform the segmentation process we followed the morphology of the cavity that could be seen in the CT scans, starting from the caudal region of the sinus within the frontal bone up to the ostium that connects the paranasal cavity to the turbinates. To determine the limit between the frontoturbinal region and the actual frontal sinus, we used the presence of the lamina that makes up the turbinates and the constriction that can be visible between the paranasal cavity and the turbinates region, which rostrally closes the frontal sinus. For the morphometric and 3D shape analysis, we chose to rely only on the left frontal sinus. Given that some fossil specimens were taphonomically deformed, we collected only individuals with at least one well preserved and undeformed sinus (if right sided, the sinus was mirrored before performing the analysis).

Morphometric variables

For each analysed specimen, we measured: maximum rostro-caudal length of the sinus (SL, in mm), volume of the left sinus (SV, in mm^3), total length of the cranium measured from prosthion to akrocranion (TL, in mm), and the occipital condyle width (OCW, in mm). This last morphometric variable has been used to estimate the body mass (BM, in kg) of each specimen according to the formula proposed in Engelman (2022). Measurements were obtained from 3D models using the software Autodesk Meshmixer (ver. 3.5.474, Autodesk). We used the natural log transformed SL, TL, BM, and the cubic root of SV (lnSL, lnTL, lnBM and lnSV) to investigate their possible covariation with the ecology of the analysed canid species. The species were grouped as in Frosali et al. (2023) and according to the ecomorphogroups defined in Van Valkenburgh and Koepfli (1993) in order to test the possible correlation between different dietary preferences and frontal sinus variables. To assess the possible presence of an allometric grade shift in lnSL and lnSV, we performed an analysis of covariance (ANCOVA) on the regression slopes obtained from ordinary least square (OLS) regressions performed on two subsamples that included hypercarnivore group-hunters+hypocarnivores and mesocarnivores+hypercarnivores on small prey, respectively.

Diffeomorphic deformations analysis

The complex and convoluted morphology of the frontal sinus is challenging for the identification of homologous landmarks on their surfaces and thus hinders the use of mainstream, landmark-based 3D geometric morphometric approaches. To better investigate the variation of these structures and the relationship of the shape variation with ecological preferences, we relied on a recently-developed technique called diffeomorphic deformation analysis (DDA), previously used by Frosali et al. (2023)

on the frontal sinus morphology of stem Canini. This kind of analysis is a landmark-free approach that allows the direct comparison between continuous surfaces based on their geometrical correspondences (Durrleman et al. 2014), which is particularly advantageous in the case of structures with a complex morphology, like in the case of the frontal sinus, because it works with previously aligned surfaces and computes the deformation magnitude and direction without considering landmarks. This is because the point-to-point correspondence used by DDA does not require strict homology, which is instead ensured by a number of preparatory steps performed prior to shape analysis (e.g., the surface alignment).

First, the surface of every left frontal sinus was reduced to 40,000 (±100) triangles using the software Meshmixer and then saved in PLY format. Following the procedure of Frosali et al. (2023), we placed a set of six landmarks that broadly describe the morphology and orientation of the frontal sinus (Online Resource 2: Fig. S1). The placement of the set of landmarks was performed in Avizo 9.0.1 (FEI Visualization Sciences Group, Houston, USA). The identified landmarks were then used to perform a General Procrustes Alignment (GPA) in R v. 4.3.3. (R Core Team 2024), using the "procSym" function of the R package "Morpho" v. 4.1.3. (Schlager 2017). The rotational matrix (describing the translation, rotation, and scaling of each set of landmarks) obtained from the GPA was used as a reference to rotate, translate, and rescale the specimens and thus ensure biological homology. We used the "computeTransform" and "applyTransform" functions of the Morpho package to apply the rotation, translation, and scaling parameter to all 3D meshes. The aligned surfaces were finally converted into ASCII legacy VTK files using the open-source software Paraview v. 5.6.0 (www.paraview.org). Because of the underdevelopment of its frontal sinus, *Vulpes lagopus* was not included in the 3D shape analysis.

The DDA was performed in the DeepFry high-performance cluster computer (LOEWE Centre for Translational Biodiversity Genomics, Frankfurt am Main, Germany) on the VTK files using the open-source software Deformetrica v. 4.3 (Bône et al. 2018) with a "Deterministic Atlas" approach and kernel size of 0.09. The DDA identified a total of 768 control points, attached to the most variable portions of the surface. The "Deterministic Atlas" first performs an additional registration of the surfaces and computes a template representing the average shape for the analysed sample. The template is then iteratively deformed towards each of the specimens included in the sample and the magnitude and direction of the deformations (momenta) are modelled by means of mathematical functions (i.e., diffeomorphisms). The output is eventually compiled by constructing an atlas of the momenta for the whole sample, also termed as deformation fields (Durrleman et al. 2014).

The deformation fields (the raw shape data obtained from the DDA) were inspected with multivariate analyses to identify the main patterns of shape variation embedded in the data. First, we performed a principal component analysis (PCA) to explore the morphospace of the canid frontal sinus. We then performed a variation of the PCA, called between group PCA (bgPCA), which relies on a PCA of the group means and allows to better highlight grouping-related shape differences (Mitteroecker and Bookstein 2011). The bgPCA was performed using the four ecomorphogroups defined by Van Valkenburgh and Koepfli (1993) (and also considered in the morphometric analyses detailed above; see Morphometric Variables) as grouping factor. The fossil specimens (*C. borjgali* D64, *C. etruscus* IGF 4407 and IGF 4412, *C. mosbachensis* IMEDEA-C2, *Eucyon adoxus* (Martin, 1973) NMB Rss.45 and *Eucyon davisi* (Merriam, 1911) F: AM 97057) were plotted a posteriori onto the morphospace to assess their group affinities with the a priori defined groups. We followed the approach defined by Cardini and Polly (2020) to ensure that the group separation observed in the bgPCA morphospace is not spurious and thus performed an additional cross-validated bgPCA. Finally, we further investigated the grouping structure of the shape data using a canonical variate analysis (CVA) and classified the specimens based on the ecomorphogroups. The CVA was performed on the first ten PCs of the PCA (68.2% of total variance) as these returned the best classification results, a commonly used practice in the analysis of highly-dimensional shape data (e.g., Zanolli et al. 2022). As in the case of the bgPCA, fossil specimens were plotted a posteriori onto the shape space.

The affinities of the individuals belonging to extinct species with the a priori defined ecomorphogroups were evaluated calculating the cross-validated posterior probabilities (for CVA scores only) and typicality probabilities of group membership (for both bgPCA and CVA scores). These two kinds of probabilities are based on different concepts. Posterior probabilities assume that each individual must belong to one of the a priori defined groups and are expressed as percentages that sum up to 100%. Conversely, typicality probabilities consider group distributions separately and indicate how "typical" the score of an individual is for each given group (Klecka 1980). They are based on the chi-square distribution and are returned as *p*-values for each group and do not sum to unity. A larger *p* is obtained when an individual is at a shorter distance from the group centroid and thus has a greater probability of belonging to the group distribution, whereas a $p < 0.05$ implies that an individual can be considered as an outlier for that group.

Phylogenetic analysis

Given the fact that the frontal sinus is a synapomorphy of the tribe Canini, we decided to investigate the phylogenetic signal in the shape variation of this structure within this taxonomic group. The Vulpini species *N. procyonoides* was thus excluded, as its developed frontal sinus is considered analogous with that of the Canini. Analyses on fossil canids (Tedford et al. 2009) indeed highlighted that this cranial feature (i.e., a well-developed frontal sinus) first appears within the stem Canini group, which it shares with the crown group, while in the genus *Nyctereutes* it appeared independently following a different evolutionary history. Furthermore, there is also a noticeable difference between *N. procyonoides* and the Canini in the portion of frontal bone that is occupied by the frontal sinus. In the latter, the frontal sinus enters within the postorbital process, whereas in *N. procyonoides* it does not (Tedford et al. 2009).

For the phylogenetic analysis, we relied on a phylogenetic tree based on the complete genomes of 31 extant South American canids (Chavez et al. 2022). The tree was used as a backbone phylogeny to which we appended the analysed extinct canine taxa based on their currently accepted phylogenetic position. Divergence times for the fossil species were arbitrarily placed 500,000 years before their first documented occurrence (Online Resource 2: Fig. S2). This methodology (i.e., adding fossil taxa to pre-existing phylogenies) was used following Urciuoli et al. (2020), where the fossil species are added 1 million years before the first documented occurrence: we chose to add them just 500,000 years before the first documented occurrence because we worked with more recent taxa that diverged in more recent times. In the case of *C. mosbachensis*, the Venta Micena site is one of the oldest and is dated to ~ 1.6 Ma (Martínez-Navarro et al. 2021). We thus placed the divergence of this species from other Canini species at 2.1 Ma. The tip for *C. mosbachensis* was placed at 0.5 Ma, coinciding with the extinction of this species (Turner 1995). The divergence from the extant species of the genus *Canis* of the recently described species *C. borjgali* (Bartolini-Lucenti et al. 2020) was placed at 2.3 Ma, based on the chronographic data for the site of Dmanisi, the only site where this species has been recognised (1.8 Ma; e.g. Ferring et al. 2011). The stratigraphic level where *C. borjgali* is present ends at around 1.76 Ma (Bartolini-Lucenti et al. 2022), which was considered as the extinction age for this species. *Canis etruscus* represents an important species in the evolutionary history of canids and is believed to have appeared in the European fossil record around 2.2 Ma, during the Early Pleistocene (Cherin et al. 2014). Its divergence with the lineage *Cuon-Canis* was thus placed at 2.7 Ma. The disappearance of *C. etruscus* is instead considered coeval with a faunal turnover that occurred at 1.4 Ma (Bartolini-Lucenti et al. 2017). Following the discussion by Tedford et al. (2009), suggesting a first diversification of the genus *Eucyon* during the Hemphillian (10.3–4.9 Ma), we placed the divergence of this taxon from the rest of the Canini at 10.8 Ma. The separation of the two species of the genus *Eucyon* here considered (i.e., *E. adoxus* and *E. davisi*) was instead placed at 9.5 Ma because the first occurrence of *E. davisi* is within the Hemphillian period (Tedford et al. 2009). The last occurrence of *E. davisi* is probably at 3 Ma (Wang et al. 2008) based on the material from Yushe Basin (Tedford and Qiu 1996), while that of *E. adoxus* is at 2.7 Ma, as testified by the lack of specimens younger than this age (Rook 2009).

To better assess the phylogenetic structure found in the shape data, we performed a newly developed PCA variant that allows maximizing the covariation of the first PCs with the phylogenetic signal, called phylogenetically aligned components analysis (PaCA; Collyer and Adams 2021). The analysis was performed on the deformation fields and phylogenetic tree using the "gm.prcomp" function of the geomorph v. 4.0.8 package for R (Adams et al. 2024) using the "align.to.phy" parameter. This approach rearranges the eigenvectors of the components of the multivariate analysis so that their covariance with the phylogeny is at its maximum. The PaCA computes the singular value decomposition of the cross-products between the matrix of the residuals and the phylogenetic covariance matrix, thus allowing maximizing the covariation between the shape variance of the first few axes and phylogenetic signal but keeping unchanged the Euclidean distances between observations in the morphospace (Collyer and Adams 2021).

The phylogenetic signal measures the degree to which related species resemble each other relative to what is expected based on their phylogenetic distance (Felsenstein 1985; Harvey and Pagel 1991), thus providing insights into the evolutionary history (e.g., neutral, convergent, and stabilizing evolution) that shaped their phenotype. To assess the phylogenetic signal embedded in the first two phylogenetically aligned components (PaCs), we used the function "phylosig" of the package "phytools" 2.3-0 (Revell 2024) and computed Pagel's λ (Pagel 1999) and Blomberg's *K* (Blomberg et al. 2003). These two metrics compare the variance observed at the tips of the phylogenetic tree to what would be expected under a Brownian motion evolutionary model (Blomberg et al. 2003; Pearse et al. 2023). Pagel's λ is a scaling coefficient that reflects the expected correlation between phylogenetically related species, ranging from 0 (no correlation and thus a lack of phylogenetic signal) to 1 (where the covariance is proportional to the phylogenetic distance, thus maxing out the phylogenetic signal). Blomberg's *K* measures how well the variance-covariance patterns found in the data match the phylogenetic tree and

shows where the variance is concentrated. This parameter can assume a wider range of values than Pagel's λ and it can be used to highlight different evolutionary patterns. In particular, a K value close to 1 suggests that the evolutionary process closely resembles what is expected under a Brownian motion model of evolution. When $K < 1$, it indicates that closely related species are less similar than expected (this means that variance is accumulated within clades). The evolutionary pattern observed in this case is not purely stochastic but is probably caused by adaptations not correlated with phylogeny (i.e., evolution of analogous structures or homoplasy). Finally, a $K > 1$ suggests that closely related species resemble each other more than expected under Brownian motion, which means that most of the variance occurs between clades. This evolutionary pattern could be indicative of a phenomenon of stabilizing selection.

Results

Among the extant species analysed in the present study, *Nyctereutes procyonoides* possesses the simplest sinus morphology (Fig. 1e). The paranasal cavity of this species lacks any kind of incision and the ventral lobe. It only presents a medial lobe that elongates rostrally from the main body of the sinus giving it a cylinder like morphology. *Cuon alpinus* (Pallas, 1811) shows instead two well-developed rostral lobes, a medial and a lateral one, with a deep incision between them (Fig. 1c). The medial lobe shows a deep sulcus on its ventral face, while on the dorsal surface there are no sulci nor incisions, not even in the posterior area of the sinus. The sinus also presents a well-developed ventral lobe, which gives the sinus a triangular shape in lateral view. In dorsal view, the expansion of the lateral lobe into the post-orbital process is noticeable. As far as the three species of the subtribe Cerdocyonina are concerned we can see a good variety of morphologies. *Atelocynus microtis* possesses two well-defined, although somewhat small, rostral lobes, a medial and a lateral one, which are separated by a wide rostral incision (Fig. 1b). The lateral lobe also shows an additional lateral incision, which defines a small lateral prominence. In lateral view (Fig. 1b), the morphology is triangular as in *Cu. alpinus* due to the presence of a well-developed ventral lobe. In this view, there is also a noticeable sulcus running alongside the medio-lateral axis at the height of the lateral sulcus (Fig. 1b). Caudally, the sinus shows another deep incision that runs parallel to the main axis of the structure, separating the caudal portion into two lobes (Fig. 1b). *Cerdocyon thous* shows a sinus morphology with two evident rostral lobes separated by a shallow rostral incision that runs alongside the main axis (Fig. 1d). The medial lobe is markedly smaller than the lateral one, reaching half of its length (Fig. 1d). The medial lobe shows an even smaller sulcus, which defines a widely medio-laterally expanded medial prominence (Fig. 1d). Due to the presence of the ventral lobe, the sinus is triangular in shape in lateral view (Fig. 1d). A small prominence is visible in lateral view, occupying the central portion of the sinus (Fig. 1d). The last South American canid, *Chrysocyon brachyurus*, shows a remarkably deep incision in the rostral portion of the sinus that divides it in two well-developed rostral lobes (Fig. 1a). The lateral lobe is also well-developed alongside the medio-lateral axis and on its most rostral portion it possesses also two small prominences (Fig. 1a). Also, the medial lobe shows a small sulcus on the medial side, running along the connection between the lobe and the main body of the sinus

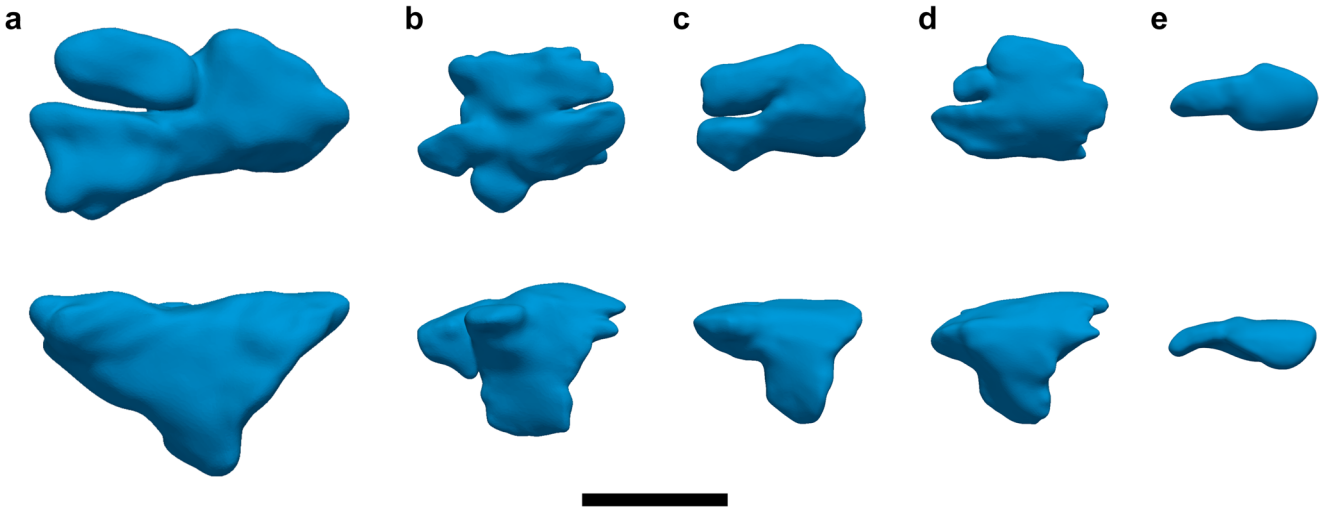

Fig. 1 Dorsal (above) and lateral (below) views of new extant species described left frontal sinuses. The rostral region is on the left in all views. **a**. *Chrysocyon brachyurus*, MAM017321; **b**. *Atelocinus microtis*, MZUF-1518; **c.***Cuon alpinus*, CBL 131; **d**. *Cerdocyon thous*, MZUF-4062; **e**. *Nyctereutes procyonoides*, USNM 255530. Scale bar equals 2 cm

(Fig. 1a). As for the previous South American species, *Ch. brachyurus* displays a triangular morphology in lateral view due to a well-developed ventral lobe (Fig. 1a).

Analysing other key features in the development and relative expansion of the frontal sinuses (namely, the rostro-caudal elongation of these paranasal cavities and their overlapping with the brain), we observe (Fig. 2) that the most rostro-caudally developed sinus is that of *Ch. brachyurus*, which partially overlaps the rostral portion of the cerebrum (Fig. 2a). The other two South American canids, *A. microtis* (Fig. 2b) and *Ce. thous* (Fig. 2d), also show a partial overlap between their sinuses and the cerebrum, but less than *Ch. brachyurus*. The other representative of the tribe Canini, *Cu. alpinus*, does not show an overlap between the sinus and the cerebrum, and the sinus is shortened rostro-caudally (Fig. 2c). The shortest sinus of them all is the one of *N. procyonoides* with a complete separation of the sinuses from the cerebrum (Fig. 2e). Another difference in this species is in the rostrally protruding sinus, being instead short in its caudal portion (Fig. 2e).

The four fossil species of the genus *Canis* show different 3D morphologies of the frontal sinus from one another (Figs. 3, 4 and 5). The frontal sinus of *Canis arnensis* (IGF 869) was highly deformed due to taphonomic processes so it was not considered in any morphometric or shape analyses and its overall 3D morphology was not clear (Fig. 3). What is visible in the left sinus is a well-developed rostrolateral lobe, while in the caudal portion some incisions are fairly visible (they might be linked to taphonomic processes; Fig. 3). In lateral view the typical triangular-like morphology of the frontal sinus is also visible, with a well-developed ventral lobe (Fig. 3). The sinus of *Canis etruscus* (IGF 4412 and IGF 4407) rostrally has only the lateral lobe which shows an incision that divides the rostral region in two smaller lobules (Fig. 4b). The rostromedial region shows instead a

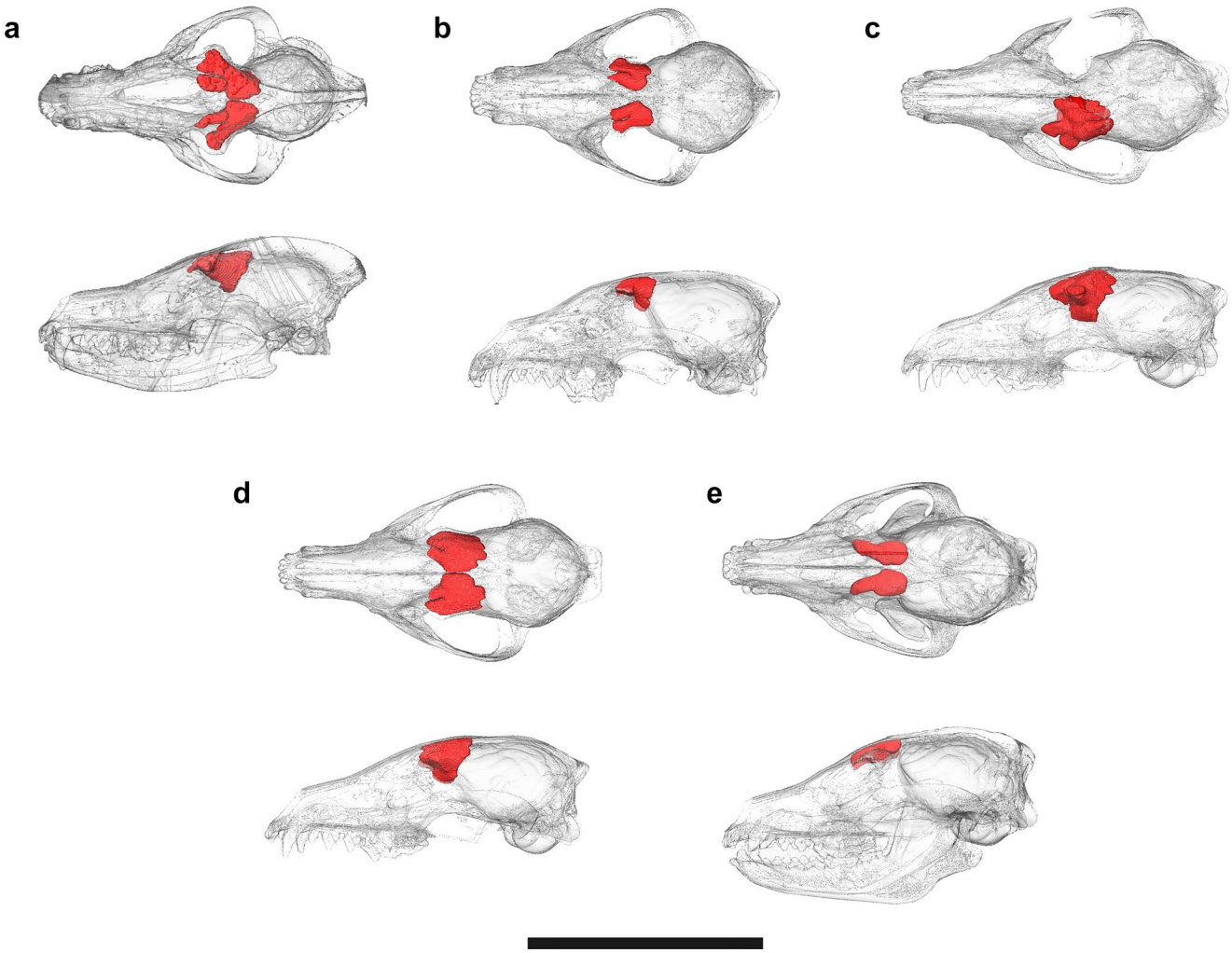

Fig. 2 Dorsal (above) and lateral (below) views of new extant species described crania and sinuses. The rostral region is on the left in all views. **a**. *Chrysocyon brachyurus* MAM017321; **b**. *Cuon alpinus* CBL 131; **c**. *Atelocinus microtis* MZUF-1518; **d**. *Cerdocyon thous*; **e**. *Nyctereutes procyonoides* USNM 255530. Scale bar equals 10 cm

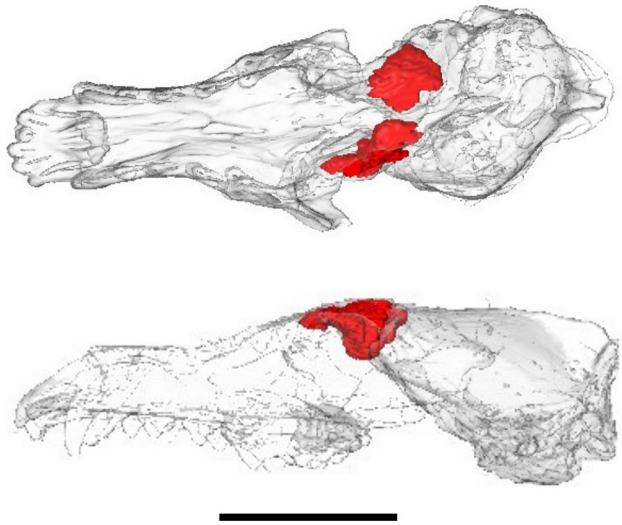

Fig. 3 Dorsal (above) and lateral (below) views of the cranium and sinus of *C. arnensis*, IGF 869. The rostral region is on the left in all views. Scale bar equals 5 cm

prominence that diverges toward the medial side; these features are absent in the IGF 4407 specimen (Fig. 4c), which only shows a developed rostrolateral lobe. The dorsal surface of IGF 4412 shows also two other sulci: one more medial and the other at the base of the rostrolateral lobe (Fig. 4b). In the IGF 4407 specimen the incision is not evident, but there is still a noticeable depression in the area at the base of the rostrolateral lobe (Fig. 4c). Despite the lack of the rostromedial lobules in the IGF 4407 specimen, it shows a more medio-laterally enlarged sinus in comparison to the other specimen of the same species (i.e., IGF 4412; Fig. 4b-c). The presence of the ventral lobe gives the sinus a triangular morphology in lateral view, and it also shows a ventrolateral prominence (Figs. 4b-c). The IGF 4407 specimen possesses a more dorso-ventrally compressed sinus in comparison to the IGF 4412 specimen, which in turn also possesses a more ventrally protruded ventral lobe (Figs. 4b-c). The rostrocaudal development of the sinus shows a partial overlap of the sinus with the rostral-most region of the brain, but the overlapping is not marked like in other extant species (e.g., *Lycaon pictus* or *Canis lupus*) and does not reach the frontoparietal suture (Fig. 5b-c). Due to the fact that the specimen IGF 4407 does not present the neurocranium it is difficult to determine the overlap of the frontal sinus with the brain, but the overall extension seems comparable with that of the other specimen of this species (i.e., IGF 4412; Fig. 5b-c). IMEDEA-C2 (i.e., *Canis mosbachensis*) shows the smallest sinus out of all the three fossil species analysed (Fig. 4d). It possesses both a rostromedial and rostrolateral lobe divided by a deep incision and with a different morphology: the lateral one is more developed than the rostromedial one (Fig. 4d). As in other species, the morphology in lateral view of the sinus is triangular, but with a more developed ventral lobe, which is more rostrocaudally enlarged than the ventral lobe of *C. etruscus* (Fig. 4b-d). Caudally, the sinus shows a few shallow incisions alongside the main axis, delimitating some caudal prominences (Fig. 4d). As in *Cu. alpinus* or *Ce. thous*, the sinus does not overlap with the cerebrum (Fig. 5d). Among the fossil species here analysed, *Canis borjgali* (D64) shows the most convoluted morphology, with one big inflated lateral lobe and one well-developed ventral lobe (Fig. 4a). The latter gives the sinus the triangular shape typical of all Canini. On the dorsal surface there is a marked dorsal sulcus that follows the medio-lateral axis, also extending on the lateral side of the sinus (Fig. 4a). Caudally, the sinus shows a deep sulcus running parallel to its main axis (Fig. 4a). This defines the medial and laterocaudal prominences, as well as the ventrolateral prominence (Fig. 4a). Between the fossil species, *C. borjgali* also shows the most rostrocaudally elongated sinus which reaches up to the frontoparietal suture (Fig. 5a).

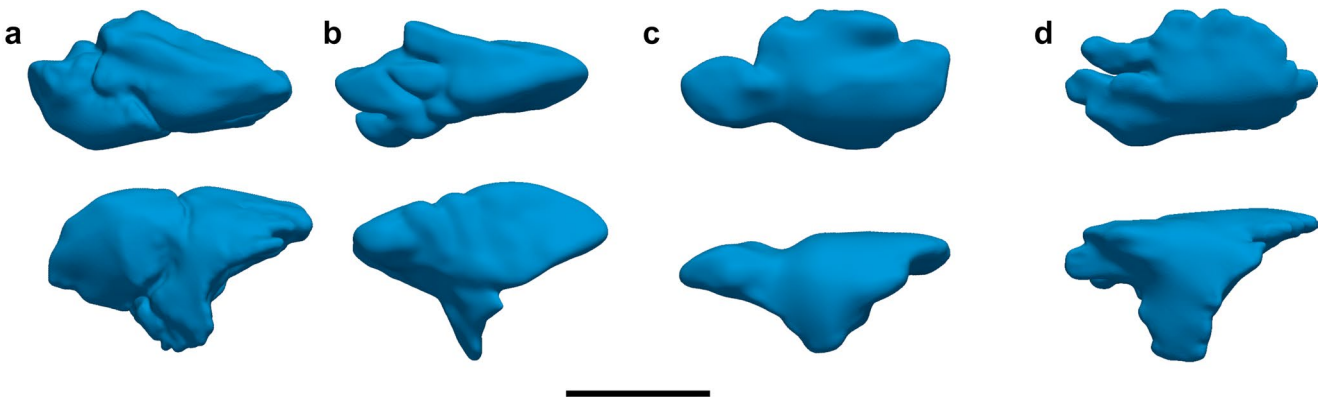

Fig. 4 Dorsal (above) and lateral (below) view of fossil species left sinuses. The rostral region is on the left in all views. **a**. *Canis borjgali* D64; **b**. *Canis etruscus* IGF 4412; **c**. *Canis etruscus* IGF 4407; **d**. *Canis mosbachensis* IMEDEA-C2. Scale bar equals 5 cm

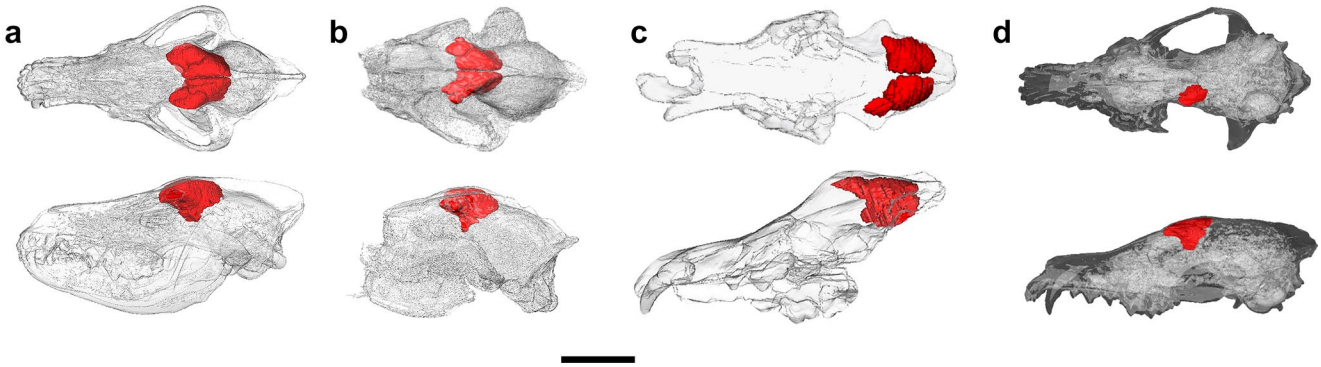

Fig. 5 Dorsal (above) and lateral (below) views of fossil species crania and sinuses. The rostral region is on the left in all views. **a**. *Canis borjgali* D64; **b**. *Canis etruscus* IGF 4412; **c**. *Canis etruscus* IGF 4407; **d**. *Canis mosbachensis*. Scale bar equals 5 cm

Morphometric comparison

The log-transformed body mass estimates and variables measured for each individual are reported in Table 1. Due to the lack of condyles in *C. mosbachensis* IMEDEA-C2 and *C. etruscus* IGF 4407, we relied on body mass estimates from literature for this species (Palmqvist et al. 1999). We relied on this body mass estimate also for *C. etruscus* IGF 4407 because the region of the occipital condyles has probably been taphonomically deformed. First, we inspected the relationship between lnSV and lnSL. Previous results by Frosali et al. (2023) showed the presence of an allometric grade shift between the ecomorphogroups of hypercarnivore group-hunters (G1) + hypocarnivores (G4) relative to mesocarnivores (G3) + hypercarnivores on small prey (G2). To validate this allometric grade shift once again, and for the extended sample analysed in the present study, we performed an ANCOVA between the aforementioned ecomorphogroup subsets. The results presented here (Fig. 6) confirm the presence of the allometric grade shift between these two groups: the two regression lines do not differ in their slope ($F=0.078$ and $p=0.781$), whereas a significant difference is noted among the intercept ($F=519.87$ and $p<<0.01$). The parameters of both regression lines are reported in Table 2. In both cases the correlation between lnSV and lnSL is strong, with the latter explaining most of the variance of the previous (85%-86.5%; Fig. 6). Out of all the fossil species here analysed, the only one that falls on the regression line of the G2+G3 is *Eucyon adoxus*, while all the other fossil specimens fall close to the regression line of G1+G4 (Fig. 6). Results also show a significant correlation between lnSV and lnSL with the lnTL and lnBM (Figs. 7 and 8). Both lnSV and lnSL show a strong and significant ($p<0.001$) correlation with cranial length (lnTL) which explains more than 70% of the total variance (Fig. 7). Both lnSL and lnSV are characterised by a positive allometry (slope lnSV-lnTL=1.50 and slope lnSL-lnTL=1.48; Table 2), meaning that species with a bigger cranium possess larger sinuses than expected. As far as body mass (lnBM) is concerned, both lnSV and lnSL show a strong and significant ($p<0.001$) correlation with it that explains a bit less than 70% of total variance (Fig. 8). In this case we instead observe a negative allometry between the sinus variables and lnBM (slope lnSV-lnBM=0.369 and slope lnSL-lnBM=0.377; Table 2), thus both the volume and the length of the sinuses grow slower than the body mass (i.e., large species possess smaller sinuses compared to small ones; Fig. 8). *Canis borjgali* falls above the regression lines in all the cases here analysed, showing the biggest similarities with G1, in particular with *C. lupus*. Conversely, *C. mosbachensis* falls above the regression lines of lnTL, while it falls under the regression lines of lnBM: in both cases it falls between the variation of G1, G2 and G3 (in particular, it closely resembles the condition of *Canis latrans*). Unfortunately, the specimens of *C. etruscus* analysed here did not preserve a complete cranium so we could not consider them in the analyses of lnTL. As far as the analyses of correlation with lnBM are concerned, we see that both specimens fall above the regression line in the case of lnSL vs. lnBM (Fig. 7a), while they fall exactly on the regression line in the case of lnSV vs. lnBM (Fig. 7b). This configuration means that *C. etruscus* possesses a longer sinus than expected in comparison to its body mass. When we consider the two fossil species of the genus *Eucyon*, *Eucyon. davisi* falls above the regression lines in all the cases here analysed, while *E. adoxus* falls under the regression lines of lnTL vs. lnSV and lnSL, while it falls on the regression lines of lnBM vs. lnSV and lnSL (Figs. 7 and 8). *Eucyon davisi* falls between the variation of *Lupulella adusta* and the G3 variation (in particular the variation of *Lupulella mesomelas* and *Canis lupaster* in the case of lnTL vs. lnSV and lnSL), while *E. adoxus* falls within the variation of G3, but also close to the variation of G2 and G1 as far as lnTL vs. lnSV and lnSL areconcerned (Figs. 7 and 8).

Table 1 Natural log-transformed morphometric variables analyzed in this study and body mass estimation. Abbreviations: **lnBM**, natural log-transformed body mass; **lnCL**, natural log-transformed cranial length; **lnSV**, natural log-transformed cubic root of sinus volume; **lnSL**, natural log-transformed sinus length

Species	ID	lnSV	lnSL	lnBM	lnCL
Atelocynus microtis	MZUF-1518	2.68	3.35	1.85	4.96
Canis aureus	CBL 299	2.60	3.47	2.19	5.10
	CBL 153	2.44	3.11	2.20	5.00
	CBL 296	2.67	3.50	2.28	5.04
	CBL 297	2.58	3.41	2.04	5.01
	CBL 298	2.54	3.46	2.19	5.07
	MZUF-11880	2.47	3.18	2.08	5.04
	016_C_GDJK	2.38	3.17	2.12	5.06
	016_C2_GDJK	2.55	3.37	2.38	5.08
	016_C3_GDJK	2.47	3.3	2.41	5.09
	MZUF-11878	2.44	3.01	2.42	5.02
Canis latrans	RD_0008	2.89	3.60	2.84	5.30
	UCLA 1225	2.68	3.38	2.59	5.24
	UCLA SO 2739	2.63	3.36	2.70	5.50
	038_C_COY	2.82	3.58	2.91	5.33
	88-50-290	2.72	3.38	2.88	5.28
Canis lupaster	MZUF-1851	2.48	3.07	1.90	5.05
	MZUF-2140	2.17	2.74	1.50	5.05
	MZUF-2110	2.19	2.91	1.62	5.01
	MZUF-2714	2.45	3.01	1.94	4.99
Canis lupus	AMNH 99667	3.20	3.86	3.31	-
	AMNH 132868	3.18	3.96	3.58	5.44
	CBL 117	3.00	3.81	3.48	5.40
	AMNH 99679	3.07	3.83	3.06	5.32
	MZUF-2032	3.08	3.96	3.36	5.39
	MZUF-11874	3.03	3.84	3.51	5.41
	037_C_WOLF	3.08	3.95	3.84	5.57
	037_C2_WOLF	2.95	3.91	3.82	5.51
	MZUF-16534	3.05	3.80	3.23	5.44
	DST-N01	2.80	3.68	3.33	5.36
Canis simensis	m-81001	2.62	3.35	3.39	5.34
	CE818	2.50	3.19	3.12	5.23
	MZUF-13781	2.66	3.36	3.41	5.32
Cerdocyon thous	MZUF-4062	2.52	3.18	1.81	4.94
Chrysocyon brachyurus	147_C_MAWO	2.92	3.52	3.4	5.32
	MAM017321	2.99	3.78	3.48	5.46
Cuon alpinus	CBL 131	2.53	3.15	3.04	5.21
Lupulella adusta	TM1942	2.45	3.32	1.73	5.04
	TM8684	2.41	3.12	2.14	5.11
	MZUF-8496	2.52	3.45	2.02	5.11
Lupulella mesomelas	UCLA 3000	2.68	3.48	2.17	5.12
	TM3028	2.45	3.14	1.82	5.00
	TM1571	2.39	3.16	1.77	5.08
	MZUF-1843	2.30	2.96	1.86	-
	MZUF-1898	2.49	3.18	1.78	5.01
	MZUF-1128	2.28	2.98	2.11	5.03
	MZUF-1715	2.59	3.29	-	4.99
	MZUF-3293	2.39	3.13	1.48	4.88

Table 1 (continued)

Species	ID	lnSV	lnSL	lnBM	lnCL
Lycaon pictus	CBL 978	2.61	3.40	2.56	5.14
	AZ11895	2.79	3.52	3.41	5.38
	AZ47678 (TM47678)	3.05	3.75	3.23	5.40
	AZTM2244	2.64	3.55	3.28	5.29
	TM5560	2.76	3.75	3.41	5.34
	USNM 368441	2.64	3.54	3.43	5.31
	368443	2.89	3.79	3.36	5.32
	MZUF-1127	2.70	3.58	3.36	5.26
Nyctereutes procyonoides	USNM 255530	2.05	3.02	1.17	4.78
	BLOC 210119	1.86	2.89	0.94	4.77
Vulpes lagopus	MZUF-1474	1.13	2.25	1.00	4.73
Canis arnensis	IGF 869	-	-	-	5.14
Canis borjgali	D64	3.08	3.82	2.99	5.39
Canis etruscus	IGF 4412	2.88	3.78	3.22	-
	IGF 4407	2.82	3.72	3.22	-
Canis mosbachensis	IMEDEA-C2	2.70	3.54	3.00	5.21
Eucyon adoxus	RSS45	2.62	3.36	2.47	5.20
Eucyon davisi	F:AM97057	2.61	3.42	2.42	5.12

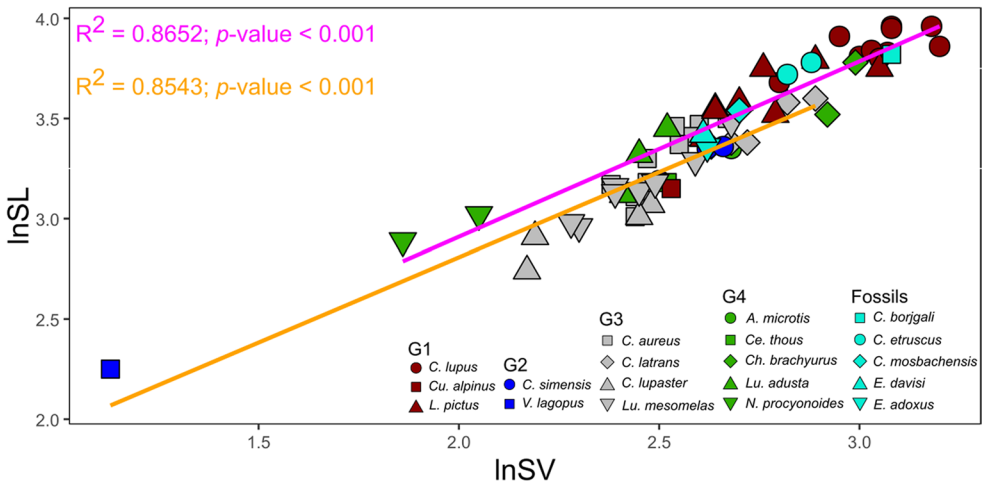

Fig. 6 Bivariate plot of natural log-transformed maximum rostrocaudal length of the left sinus (lnSL) vs. natural log-transformed cubic root of sinus volume (lnSV), with two regression lines based on two subsets composed by the following ecomorphogroups: G1 (hypercarnivorous group-hunters) + G4 (hypocarnivores), represented by the pink regression line; G2 (hypercarnivores on small prey) + G3 (mesocarnivores), represented by the orange regression line. Species are colored according to the ecomorphogroups of Van Valkenburgh and Koepfi (1993)

Table 2 Results of the ordinary least squares regressions computed for the analyzed morphometric variables of the frontal sinus. For the regression of lnSL vs lnSV, we report the results for two separate regressions obtained for two subsets of ecomorphogroups (hypercarnivorous group-hunters-G1 + hypocarnivore-G4; hypercarnivores on small preys-G2 + mesocarnivores-G4). Significant *p*-values are in bold

	R^2	*p*-value	Slope	Std. error	95% Confidence Interval	Intercept	Standard error	95% Confidence Interval
lnSL vs. lnSV (G2+G3)	**0.854**	**<0.001**	**0.850**	**0.064**	**0.719–0.980**	**1.108**	**0.159**	**0.783–1.434**
lnSL vs. lnSV (G1+G4)	**0.865**	**<0.001**	**0.875**	**0.066**	**0.739–1.012**	**1.160**	**0.185**	**0.780–1.539**
lnSV vs. lnTL	**0.727**	**<0.001**	**1.500**	**0.119**	**1.261–1.739**	**-5.150**	**0.618**	**-6.388–-3.913**
lnSL vs. lnTL	**0.715**	**<0.001**	**1.478**	**0.120**	**1.237–1.718**	**-4.251**	**0.622**	**-5.496–-3.006**
lnSV vs. lnBM	**0.665**	**<0.001**	**0.369**	**0.033**	**0.304–0.435**	**1.667**	**0.089**	**1.489–1.845**
lnSL vs. lnBM	**0.680**	**<0.001**	**0.377**	**0.032**	**0.312–0.441**	**2.428**	**0.088**	**2.252–2.603**

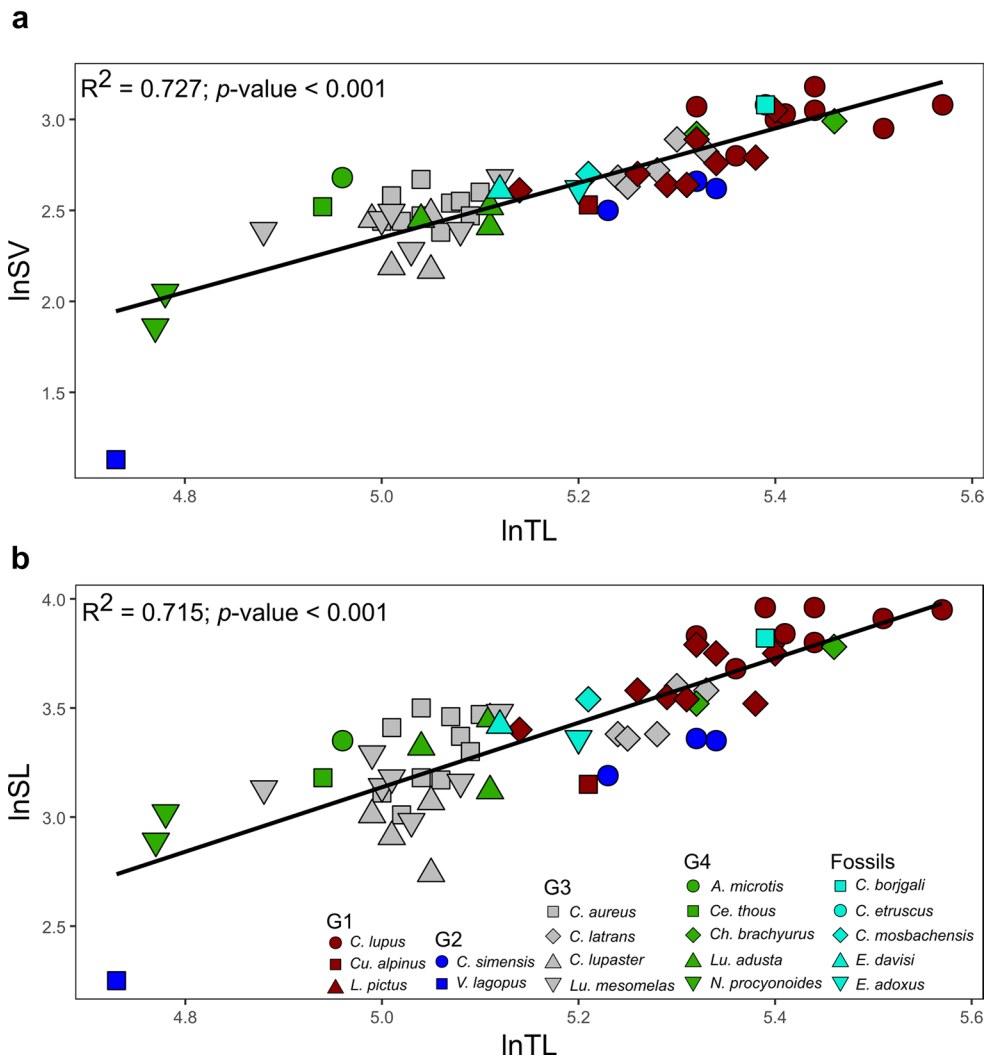

Fig. 7 Natural log-transformed bivariate plots of **a**. the cubic root of sinus volume (lnSV) versus cranial length (lnTL); **b**. maximum rostro-caudal length of the left sinus (lnSL) and cranial length (lnTL). Lines represent the ordinary least square regressions best-fit lines for the whole canid sample, which shows a significant correlation between all the variables. Species are colored according to the ecomorphogroups of Van Valkenburgh and Koepfli (1993)

Diffeomorphic deformations analyses

Grouping structure in the shape data

The results of the PCA performed on the shape data did not separate well the different ecomorphogroups (Online Resource 1: Tables S3-S4; Online Resource 2: Fig. S3-S4; Online Resource 3: Supplementary Text). To better assess the most relevant morphological features in frontal sinus shape, we also performed bgPCA and CVA analyses (the latter presented in Online Resource 1: Tables S5-S6-S7-S8; Online Resource 2: Fig. S5; Online Resource 3: Supplementary Text). The results of the bgPCA analysis allow for a good classification of the individuals in the four ecomorphogroups, with 84.5% of correctly classified individuals (Table 3; the results of the cross-validated bgPC scores are instead reported in Online Resource 1: Table S9; Online Resource 2: Fig. S4; Online Resource 3: Supplementary Text). The bgPC1 (62.2% of variance) allows to distinguish between G1 and G3 (although with limited overlap), where the species belonging to the first group show negative values of this axis (with the exception of two individuals of *C. lupus*) while the species of the latter group possess positive values of bgPC1 (with the exception of one individual of *Canis aureus* and one of *Lu. mesomelas*; Fig. 9a-b). The species belonging to G4 show more intermediate bgPC1 values, like the species belonging to G2 (Fig. 9a-b). The positive values of bgPC1 are associated to a slenderer morphology of the sinus, with a mainly developed rostrolateral lobe, while negative values of this axis are associated with a

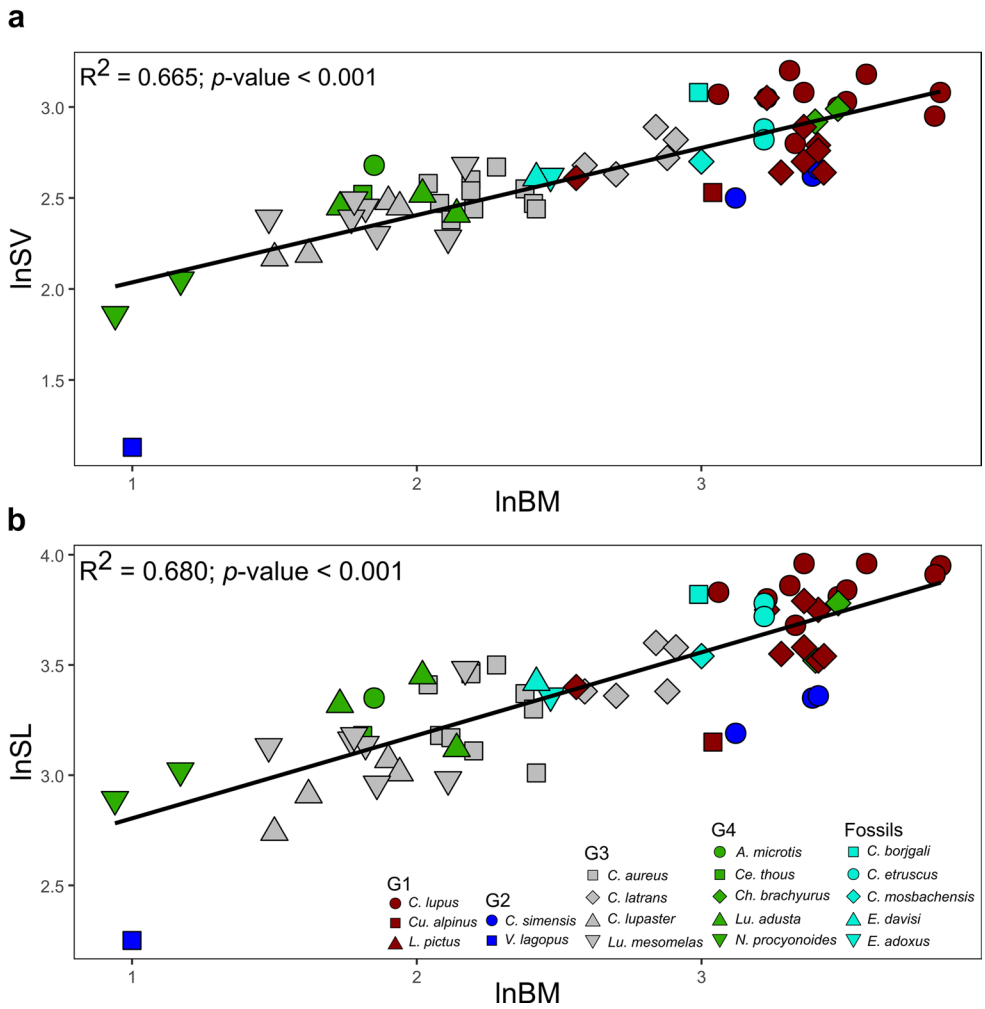

Fig. 8 **a**. Bivariate plot of the natural log-transformed cubic root of sinus volume (lnSV) and natural log-transformed body mass (lnBM); **b**. Bivariate plot of the natural log-transformed maximum rostrocaudal length of the left sinus (lnSL) and natural log-transformed body mass (lnBM). Lines represent the ordinary least square regressions best-fit lines for the whole canid sample, which shows a significant correlation between all the variables. The species are colored according to the ecomorphogroups of Van Valkenburgh and Koepfli (1993)

Table 3 Classification results obtained with a between-group principal component analysis performed on the raw shape data obtained from the frontal sinus diffeomorphic deformation analysis. **G1**, hypercarnivorous group-hunters; **G2**, hypercarnivores on small preys; **G3**, mesocarnivores; **G4**, hypocarnivores

	G1	G2	G3	G4
G1	84.2%	0%	10.5%	5.26%
G2	0%	100%	0%	0%
G3	3.70%	3.70%	88.9%	3.70%
G4	0%	0%	33.3%	66.7%

more medio-laterally enlarged sinus with equally underdeveloped rostral lobes (Fig. 9c). Alongside bgPC2 (23.83% of variance), G1 and G3 are less distinguished, because they both occupy the positive and moderately negative range for this axis. bgPC2 values only clearly separate G2, as it falls on marked negative values, whereas G3 largely overlaps with G1 and G4 on moderately negative scores (Fig. 9a). Positive values of this axis correspond to a sinus morphology that lacks a rostral incision and that presents only a well-developed rostro-lateral lobe (Fig. 9c). On the contrary, negative bgPC2 scores are associated to a deep and wide rostral incision with two well-developed rostral lobes (Fig. 9c). Finally, G1 and G3 are not well-distinguished alongside bgPC3, overlapping on intermediate values (Fig. 9b). G2 and G4 are instead found at the extremes, with the first group that possesses more positive scores for this axis, while G4 lays at the negative end of the bgPC3 values (Fig. 9c). The shape changes driving this axis are mainly associated with the morphology of the rostral lobes, so that positive values of bgPC3 are associated with the possession of one well-developed and inflated rostrolateral lobe and one underdeveloped rostromedial lobe, while the negative values are associated with a well-developed yet less inflated rostrolateral lobe and a divergent rostromedial lobe (Fig. 9c). As far as the fossil

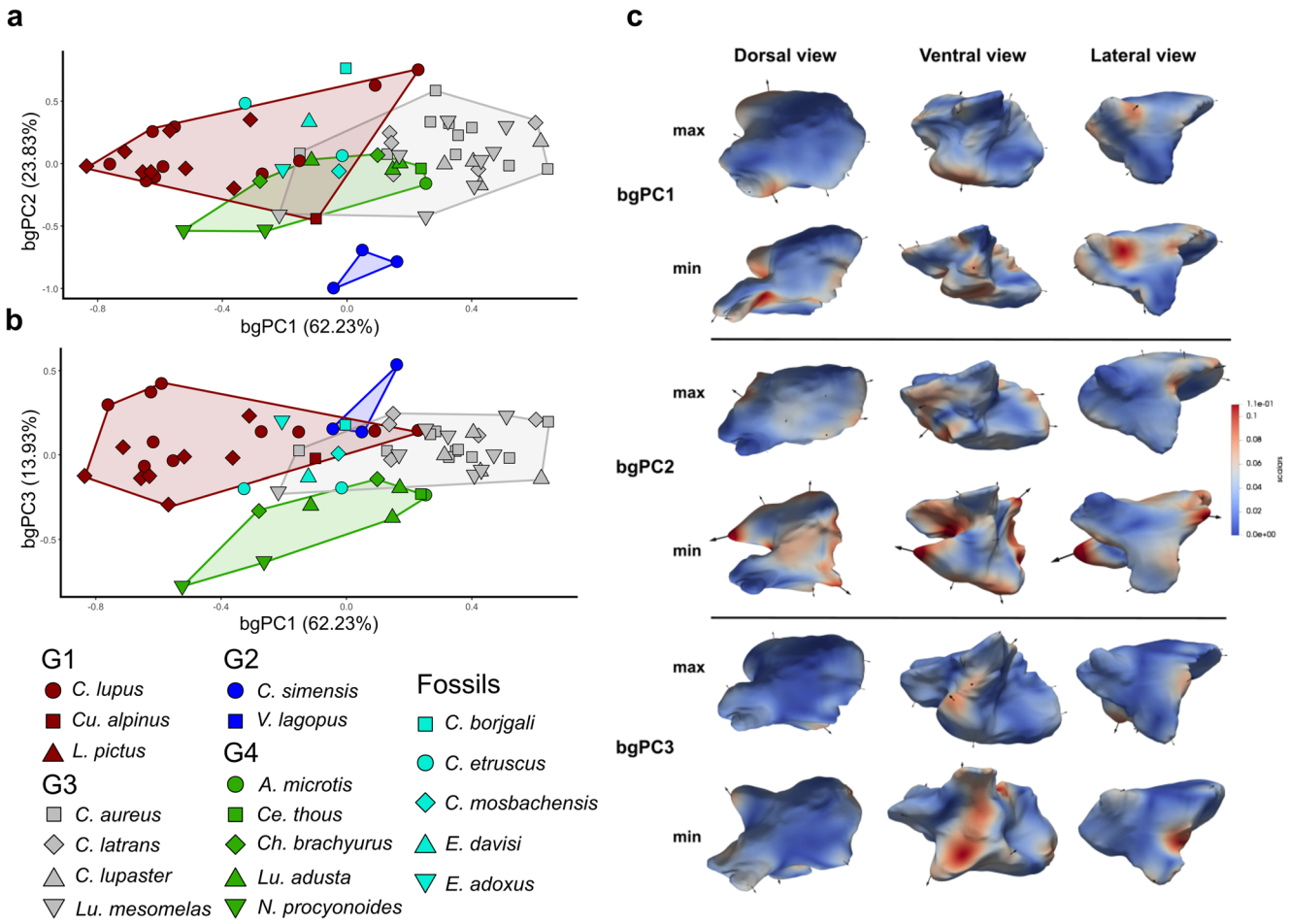

Fig. 9 a-b. Bivariate plots of bgPC2 vs. bgPC1 (**a**) and bgPC3 vs. bgPC1 (**b**); **c**. maximum (above) and minimum (below) extreme conformations of shape variation of the first three bgPCs. Cumulative deformations from mean shape are mapped on the surfaces by means of a pseudocolor scale ranging from dark blue (no displacement) to dark red (0.11 mm). Black arrows correspond to the vectors identifying the direction and magnitude of displacement. Convex hulls showing the distribution are colored as follows: dark red, hypercarnivorous group-hunters (G1); blue, hypercarnivores on small preys (G2); grey, mesocarnivores (G3); green, hypocarnivores (G4)

Table 4 Typicality probabilities based on the bgPCA scores for the considered groups computed for the analyzed fossil specimens (values < 0.05 imply that the specimen is an outlier for the ecomorphogroup). The highest non-significant value for each specimen is in bold. Ecomorphogroup abbreviations: **G1**, hypercarnivorous group-hunters; **G2**, hypercarnivores on small preys; **G3**, mesocarnivores; **G4**, hypocarnivores

	G1	G2	G3	G4
C. etruscus (IGF 4412)	0.038	<0.001	<0.001	0.005
C. etruscus (IGF 4407)	0.040	<0.001	**0.296**	**0.683**
C. borjgali (D64)	0.037	<0.001	0.002	<0.001
C. mosbachensis (IMEDEA-C2)	**0.156**	<0.001	**0.561**	**0.134**
E. davisi (F: AM97057)	**0.119**	<0.001	0.047	**0.094**
E. adoxus (NMB Rss.45)	**0.437**	<0.001	**0.053**	0.001

species are concerned, *C. borjgali* falls outside the variation of all the extant ecomorphogroups when we consider bgPC1 and bgPC2 at the same time (Fig. 9a), while it falls within the variation of G1 and G2 when we consider bgPC1 and bgPC3 (Fig. 9b). One of the two individuals of *C. etruscus* falls outside the variation of all extant ecomorphogroups, but close to the convex hull of G1, while the other *C. etruscus* falls within the variation of G4 and G3 (Fig. 9a-b). The last fossil species of the genus *Canis*, *C. mosbachensis*, falls mainly within the variation of G1 and G3 and, when we consider bgPC2, also within the variation of G4 (Fig. 9a-b). Finally, as far as the two species of the genus *Eucyon* are concerned, we see that *E. davisi* falls within the variation of G1 (Fig. 9a) and G3 (Fig. 9b), while *E. adoxus* falls mainly within the variation of G1 (Fig. 9a), yet it shows affinities with G3 (for bgPC2 and bgPC3; Fig. 9a-b) and G2 (when we consider bgPC3 alone; Fig. 9b).

Table 4 shows the typicality probabilities computed for each fossil species here analysed (the specimen is an outlier for the a priori defined group if the value is inferior to 0.05). *Canis etruscus* IGF 4412 and *C. borjgali* are outliers for all the extant ecomorphogroups. In turn, the other individual of *C. etruscus* (IGF 4407) shows the highest probability of

belonging to G4 and it can be considered as an outlier for G1 and G2; *C. mosbachensis* is recovered as an outlier only for G2, while it presents the highest typicality probability for G3. Finally, *E. davisi* and *E. adoxus* are classified as belonging to G1, with the former that can be considered as an outlier for G2 and G3 and the latter for G2 and G4.

To evaluate the role of lnBM, lnSL and lnSV on the bgPCs we performed a bivariate regression between these variables and the first three bgPCs (Table 5). All the bgPCs show a significant correlation with all the parameters, except for bgPC2 and lnBM. Although significant, the correlations are generally weak ($R^2 < 0.40$), with the most relevant ones being those between bgPC1 and lnBM ($R^2 = 0.32$) and between bgPC1 and lnSL ($R^2 = 0.36$). Overall, even if some shape differences might be partly driven by size, the latter does not play a major role in shaping ecologically-relevant morphological differences.

Phylogenetic analysis

To better investigate the phylogenetically relevant differences in the shape changes we observed in canids frontal sinuses, we performed a PaCA based on the shape data obtained from the DDA and a phylogeny for the analysed taxa. The first two PaCs explain almost 97.5% of total covariance with the phylogenetic signal, even if the RV is extremely low (cumulative RV of the first two PACs: 0.0239). The first axis (PaC1, 87.7% of covariance) discriminates between the tribe Canini and the genus *Eucyon*, which is considered to be basal to this clade of the family Canidae (Fig. 10a). The morphology of the sinus associated with the extreme values of this axis are shown in Fig. 10b. The positive values of PaC1 are associated with a different development of the rostral lobes, so that the rostrolateral lobe is markedly more developed than the rostromedial one. The negative values are instead associated with a more medio-laterally enlarged sinus morphology and the two rostral lobes are comparable in rostro-caudal extension (the rostrolateral one is slightly more developed and complex than the rostromedial one in this case as well; Fig. 10b). Hence, the extension of the rostrolateral lobe represents a good phylogenetic discriminator, differentiating the genus *Eucyon* (with a slenderer morphology of this lobe, and of the overall sinus morphology) from the rest of the tribe Canini (showing a more medio-laterally enlarged rostrolateral lobe; Fig. 10b). Another phylogenetically relevant character is the relative size of the rostromedial lobe, for which the tribe Canini tends to have a larger rostromedial lobe in comparison to *Eucyon*. PaC2 (9.52% of covariance) is instead able to discriminate between the subtribes of Canini: Cerdocyonina occupies the positive end for this axis, while Canina mainly occupies negative values (Fig. 10a). Positive PaC2 values are associated with a rostro-caudally shortened sinus that shows also a caudal incision on the dorsal surface and a medially divergent rostro-medial lobe, while the negative side of the axis is associated to a more rostro-caudally elongated sinus morphology, with no caudal incision or constriction and two parallel well-developed rostral lobes (Fig. 10b). The results of the phylogenetic signal for the two PaCs are reported in Table 6, and they are coherent with what is shown in the PaCA (we chose to report only the first two PaCs because the third one does not present any significant phylogenetic signal and explains an extremely small percentage of the total covariance). Both Pagel's λ and Blomberg's *K* are significant for the two PaCs. The values of Pagel's λ are close to 1 for both axes, thus indicating species distribution in the morphospace is similar to that based on Brownian motion (BM) expectations. Blomberg's *K* value shows some deviations (although limited) from unity for PaC1 (>1) and PaC2 (<1). These results imply that closely phylogenetically related species tend to be more similar than expected on BM when shape changes captured by PaC1 are considered, whereas the opposite applies for PaC2. Although slightly in contrast with the results of Pagel's λ, Blomberg's *K* values suggest the presence of some stabilizing selection regarding the development of rostral lobes. By plotting the phylogenetic tree onto the morphospace identified by the PaCA, we can intuitively visualize the magnitude and direction of evolution within the shape space. The stem Canini group (here represented by the genus *Eucyon*) shows a completely

Table 5 Results of ordinary least squares regressions of bgPC1-3 against sinus morphometric variables performed to assess the effect of size on shape. Regressions with significant *p*-values are in bold

	R^2	*p*-value	Slope	Std. error	95% Confidence Interval	Intercept	Std. error	95% Confidence Interval
bgPC1 vs. lnBM	**0.316**	**<0.001**	**-0.319**	**0.059**	**-0.437–-0.202**	**0.825**	**0.160**	**0.506–1.145**
bgPC2 vs. lnBM	-0.010	0.540	0.036	0.058	-0.081–0.153	-0.071	0.159	-0.389–0.247
bgPC3 vs. lnBM	**0.159**	**< 0.001**	**0.129**	**0.036**	**0.057–0.201**	**-0.341**	**0.098**	**-0.538–-0.144**
bgPC1 vs. lnSV	**0.170**	**<0.001**	**-0.618**	**0.166**	**-0.949–-0.286**	**1.627**	**0.442**	**0.743–2.511**
bgPC2 vs. lnSV	**0.151**	**<0.001**	**0.480**	**0.137**	**0.206–0.754**	**-1.248**	**0.365**	**-1.978–-0.517**
bgPC3 vs. lnSV	**0.166**	**<0.001**	**0.339**	**0.092**	**0.155–0.524**	**-0.902**	**0.246**	**-1.393–-0.411**
bgPC1 vs. lnSL	**0.359**	**<0.001**	**-0.796**	**0.132**	**-1.061–-0.532**	**2.715**	**0.455**	**1.806–3.624**
bgPC2 vs. lnSL	0.138	0.002	0.417	0.125	0.167–0.668	-1.405	0.431	-2.266–-0.544
bgPC3 vs. lnSL	0.055	0.035	0.192	0.090	0.014–0.370	-0.660	0.306	-1.272–-0.048

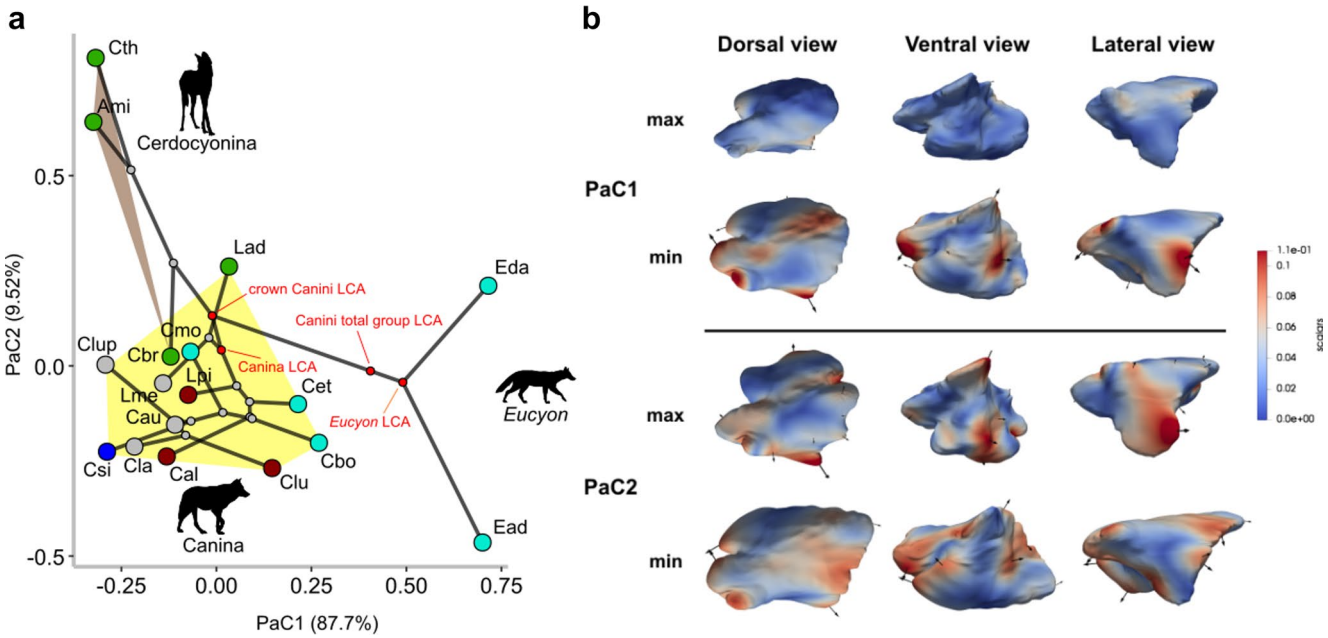

Fig. 10 **a**. Bivariate plot of PaC2 vs. PaC1 with the phylogeny projected on the morphospace. The convex hulls correspond to Cerdocyonina (brown) and Canina (yellow); **b**. Maximum (above) and minimum (below) extreme conformations of shape variation of the first two PaCs. Cumulative deformations from mean shape are mapped on the surfaces by means of a pseudocolor scale ranging from dark blue (no displacement) to dark red (0.11 mm). Black arrows correspond to the vectors identifying the direction and magnitude of displacement. Species abbreviations: **Ami**, *A. microtis*; **Cau**, *C. aureus*; **Cbo**, *C. borjgali*; **Cet**, *C. etruscus*; **Cla**, *C. latrans*; **Clup**, *C. lupaster*; **Clu**, *C. lupus*; **Cmo**, *C. mosbachensis*; **Csi**, *C. simensis*; **Cth**, *Ce. thous*; **Cbr**, *Ch. Brachyurus*; **Cal**, *Cu. Alpinus*; **Ead**, *E. adoxus*; **Eda**, *E. davisi*; **Lad**, *Lu. Adusta*; **Lme**, *Lu. Mesomelas*; **Lpi**, *L. pictus*

Table 6 Pagel's λ and Blomberg's *K* computed for the first two components (PaCs) of the phylogenetically-aligned component analysis performed on the species shape averages. Both show a significant ($p < 0.05$) phylogenetic signal

	Pagel's λ	*p*-value	Blomberg's K	*p*-value
PaC1	0.821	0.002	1.43	0.007
PaC2	1.00	0.002	0.713	0.028

different evolutionary trajectory from the crown group. Within the crown-Canini, *Lu. adusta* appears to be the most primitive and close to the reconstructed last common ancestor (LCA) morphology of the tribe. Among the Cerdocyonina, *A. microtis* and *Ce. thous* diverged broadly from their LCA due to the possession of a rostro-caudally shortened sinus morphology, with a caudal incision and a small divergent rostromedial lobe, whereas *Ch. brachyurus* converged with the Canina. This latter subtribe shows a tight clustering of both the phylogeny tips and ancestral nodes. This further suggests the presence of a quite evolutionary stable morphology in this group (although not particularly close to that of the estimated LCA), yet with some interesting trends within the group. Particularly, *C. lupus* seems convergent with both the extinct species *C. etruscus* and *C. borjgali* by the presence of a highly developed rostrolateral lobe and additional dorsal incision on the surface of the sinus. Conversely, even if with some differences, the remaining taxa of the Canina evolved in the same way relative to the LCA of the subtribe, showing some similarities with *Ch. brachyurus* in the medio-lateral enlargement of the rostrolateral lobe, that is also less rostrally protruded and comparable in dimensions to the rostromedial one.

Discussion

Frontal sinuses are important endocranial cavities, from both a phylogenetic and ecological point of view, even if the main ecological factor that drives the development of these structures in Caninae is still not clear. In other carnivorans these cavities have been more deeply investigated, such as in hyaenids (Joeckel 1998; Vinuesa et al. 2015, 2016; Vinuesa 2018) and borophagines (Tseng and Wang 2010), two groups considered ecological homologous that have evolved in different continents (the first in Eurasia, the latter in North America; Wang et al. 2008). Both groups show adaptations towards a durophagous diet, which likely led to the convergent evolution of domed crania and highly developed sinuses (Tseng and Wang 2010; Vinuesa et al. 2016). These data on duraphagous extant (i.e., hyaenas) and fossil (i.e., borophagines) species thus suggest that the frontal sinus evolved at least twice, likely in response of selective pressures related to diet and dispersion of stresses and strains

during feeding. Furthermore, the size of this endocranial cavity appears to be correlated with the hardness of the food eaten (the tougher the food item, the larger the frontal sinus; Curtis and Van Valkenburgh, 2014). Such results corroborate the feeding hypothesis that frontal sinus morphology in carnivorans is related to the diet of the species, in particular to the hardness of the food eaten, which has been proven within the Caninae family by previous works that correlated the frontal sinus structure to the dispersion of stresses during feeding (Frosali et al. 2023, Peri et al. 2025). Even if the covariation between frontal sinus variation and diet holds up within Caninae, other ecological factors (Joeckel 1998; McGreevy et al. 2004; Vinuesa et al. 2015, 2016; Vinuesa 2018; Pérez-Ramos and Figueirido 2020) can intervene in shaping this endocranial cavity and cannot be entirely ruled out. On top of that, although diet and other ecological functions are the main drivers for the presence/absence and morphology of a frontal sinus, such functional signal cannot be entirely separated from the phylogenetic relevance of this character, which serves well to discern between Caninae tribes (i.e., the tribe Vulpini does not possess the frontal sinus, while the tribe Canini do).

The frontal sinuses in fossil *Canis* species from the Early Pleistocene: the role of ecology

The fact that sinus morphology is driven not only by ecology or phylogeny, but rather by a combination of both, is clearly evinced from the results presented above (especially, the fact that a member of Vulpini like *Nyctereutes procyonoides* secondarily evolved this structure is a clear hint for the role played by ecology in the development of this paranasal cavity). Regarding the influence of ecology on sinus morphology, we here observe that the extant ecomorphogroups are well-defined in terms of sinus morphology and relative features: G1 is characterised by a rostrally protruded rostrolateral lobe, which corresponds to a more rostro-caudally developed sinus morphology, G2 shows an equal development of the rostral lobes, with a deep and wide incision to separate them and G3 tends to have a medio-laterally enlarged sinus with relatively less rostrally developed rostral lobes (Fig. 9) The group with the least distinctive sinus morphology is G4. Indeed, this cluster includes a wide variety of taxa from different tribes (both Vulpini and Canini) and subtribes (both Cerdocyonina and Canina), which underwent different evolutionary histories, particularly, *N. procyonoides* (see paragraph 4.2). This is also testified by the removal of *N. procyonoides* from the PCA, resulting in a narrowed morphological variation for this ecomorphogroup (G4; Online Resource 2: Fig. S4). Furthermore, the bgPCA showed a good degree of classification of the species with the different ecomorphogroups well-separated from one another, with the only exception of the less well-defined G4 for the reasons mentioned above (Table 6). The uncertainty in correctly classifying species in the G4 group is further exemplified by the results of the cross-validated bgPCA. Indeed, this shows that bgPC3 scores (for which G4 appears most distinctive) might be affected by exaggerated group separation (Online Resource 2: Fig. S5b). This might be the result of spurious grouping caused by the bgPCA approach applied to small and differently sized groups, as was highlighted by Cardini and Polly (2020), so that the separation is caused by the method rather than being found in the shape data. Furthermore, the CVA did not present a high degree of classification accuracy for the considered ecomorphogroups (Online Resource 1: Table S5). The introduction of a higher number of species for each group in comparison to Frosali et al. (2023) showed a higher-than-expected variation of the sinus morphology for each ecomorphogroup and this caused a higher overlap than what was previously seen.

Our results also show that a better understanding of the impact of ecology on frontal sinus size and morphology must take into account the rostrocaudal development and volume of the sinus. Indeed, when these morphometric variables (lnTL, lnSL, lnSV) were analysed while accounting for the species body mass (lnBM), we identified a clearer separation between the ecomorphogroups than what we see just looking at the overall morphology of the cavity. In particular, the analyses here performed showed that the allometric grade shift between G1 + G4 and G2 + G3, already noticed in Frosali et al. (2023), holds true even after the introduction in the dataset of additional extant and extinct species. This difference between the two subsets of ecomorphogroups might be linked to the hardness of the food processed in the diet of the various species: in particular, G1 and G4 species tend to encounter more stresses during feeding (G1 species hunts large prey, more difficult to take down, while G4 have an hypocarnivorous diet that consist also of hard food), thus causing a greater development of the frontal sinus.

By analyzing the sinus morphology of three fossil species of the genus *Canis* we obtained insights into the past morphological variation of this genus. Among them, *C. etruscus* is reconstructed to be the most primitive in terms of sinus morphology, confirming its morphological and phylogenetic interpretations (Torre 1967; Tedford et al. 2009; Brugal and Boudadi-Maligne 2011; Cherin et al. 2014; Bartolini-Lucenti 2020). The primitiveness of *C. etruscus* is evident in the retention of the plesiomorphic condition for the subtribe Canina (i.e., corresponds to a sinus with one main rostrolateral lobe developed and a rostromedial one absent or underdeveloped). The phylogenetic analysis might also suggest another hypothesis, which would entail the reversal of the plesiomorphic condition (Fig. 10). We consider this hypothesis less

parsimonious as it would imply a first development of a rostromedial lobe within the tribe Canini in the ancestors of *C. etruscus* (not yet discovered) and then a secondary loss of this same lobe in *C. etruscus*. Furthermore, it has to be considered that we placed *C. etruscus* on the most common accepted phylogenetic position (i.e., closely related to the evolutionary lineage of *Canis*), but being one of the oldest species of the genus *Canis* to live in Europe (Rook and Torre 1996), it might actually belong to another clade, and possibly be closely related to other extant and more ancient lineages of extant canids, thus better explaining its primitive frontal sinus morphology. On the other hand, *C. mosbachensis* shows the most derived morphology among the three fossil species (with *C. borjgali* being more primitive due to a sinus morphology that is close to that of the inferred Canini total group LCA). This again fits with the current evolutionary and morphological interpretation of *C. mosbachensis*, suggesting that it represents the most derived fossil species out of the five here analysed, while *C. borjgali* and *C. etruscus* are considered as more primitive (Bartolini-Lucenti et al. 2017; Bartolini-Lucenti 2020; Martínez-Navarro et al. 2021). In comparison to extant taxa of grade-*Canis*, it is interesting to note that *Eucyon davisi* displays the plesiomorphic condition (i.e., the presence of a single lobe, the rostrolateral one, in the rostral region of the sinus), which is also shared by *Lupulella adusta* and *C. etruscus*. *Lupullella mesomelas*, despite being interpreted as congeneric of *Lu. adusta* by the majority of the scholars (though not all, e.g., Zrzavý and Řičánková 2004), not only possesses a rostrolateral lobe, but also a rostromedial one. This is a more derived feature, which possibly evolved due to ecological pressures related to the mesocarnivorous diet of this species. Van Valkenburgh and Koepfli (1993) describe this ecomorphogroup (i.e., G3) as capable of seldomly hunting down large prey, as testified from the proportionally robust mandible corpus as well as other cranial and dentognathic proportions to resist wrestling and struggling prey, thus suggesting some similarities with hypercarnivore group-hunters. The primitive morphology of the frontal sinus with one rostro-lateral lobe persists also in *Lycaon pictus*, the first taxon to split from the clade *Lycaon-Cuon-Canis* (e.g., Lindblad-Toh et al. 2005; Chavez et al. 2022). This species possesses a frontal sinus with one lobe, but generally more inflated and sub-lobed. In the derived species of this clade the sinus develops the two rostral lobes, until the most derived condition represented by *Canis lupus* where the cameration reaches its peak and it is evident also the presence of many different sulci. The derived morphology of the sinus (i.e., two main rostral lobes) is also evident in the South American canids, and probably it was developed as a convergent adaptation because of the hypocarnivorous diet of these species, highlighting once again the double drivers in the morphology of this paranasal cavity. All of the three fossil species of the genus *Canis* possess sinuses whose dimensions fall in the range of variation of G1, G3 or even G4. It is thus not possible to disentangle the diet of these fossil species by only considering the dimensions and morphology of their frontal sinuses. This is particularly relevant if we consider the fact that extant ecomorphogroups are probably representing a smaller portion of the variation shown by Canidae ecomorphogroups in the past, as Van Valkenburgh (1989) suggested. It must be remembered that extant ecomorphogroups (and thus their range of ecomorphospace variation) might actually be the only surviving types of a much wider spectrum of trophic and adaptive ecologies that existed in the past (Van Valkenburgh 1989, 2007; Van Valkenburgh et al. 2003; Friscia et al. 2007; Bartolini-Lucenti and Rook 2021). However, the dimensions of the analysed fossil species frontal sinuses suggest that these canids were able to resist important stresses during their feeding process. The two individuals of *Canis etruscus* show frontal sinuses that are remarkably similar with those of extant hypocarnivores and hypercarnivore group-hunters. Based on its peculiar dentition, the diet of *C. etruscus* was probably hypocarnivorous-like. Coupled with its large body mass, this evidence suggests an ecological niche more similar to that of *Chrysocyon brachyurus* than to that of *Lu. adusta*, regardless of the large phylogenetic distance between *C. etruscus* and *Ch. brachyurus* (indeed, our shape analyses recover one of the two individuals close to *Ch. Brachyurus*). We must take into account that *C. etruscus* shared its habitat with other two canids, *Xenocyon falconeri* and *Canis arnensis*, so that its well-specialised diet might have represented an evolutionary advantage as it allowed *C. etruscus* to occupy a different ecological relative to its contemporaries, and thus better coexist with other canid fossil species during the Pleistocene (Cherin et al. 2013). In particular, according to some authors (e.g., Flower and Schreve 2014), the enhanced crushing capabilities and shorter/narrower carnassial blades would reflect a higher proportion of non-flesh foods in the diet. The sinus development and similarities with hypocarnivores morphology seem to corroborate this hypothesis. Still according to Flower and Schreve (2014), differences in the dentition between *C. mosbachensis* and *C. etruscus* are evident, thus implying a clear dietary difference between the two species. In particular, *C. mosbachensis* presents reduced upper molars and a shallower jaw, suggesting that this species had a less carnivorous diet than the extant wolf and it was possibly capable of hunting down only small preys (Meloro 2011; Flower and Schreve 2014). The

Mosbach wolf was further differentiated by *C. lupus* and *C. etruscus* by its reduced crushing capabilities and potential increased slicing ability indicated by elongated upper carnassials, thus suggesting a more hypercarnivorous diet than *C. etruscus* and a more specialised feeding habits than *C. lupus* (Flower and Schreve 2014). The analyses on frontal sinus shape performed here support this idea. Indeed, *C. mosbachensis* falls close to the variation of G1 (Fig. 9 and Online Resource 2: Fig. S4), but not particularly close to the wolf one.

Finally, as far as *C. borjgali* is concerned, its dietary preferences are not still well-characterised, but previous analyses (e.g., Bartolini-Lucenti et al. 2020, 2022) showed that this species presents more derived features than *C. etruscus* and *C. arnensis* and seems to be closely related to *C. mosbachensis* from an evolutionary point of view. The frontal sinus of this species shows a few similarities with the wolf and hypercarnivorous group-hunters, although in most of the analyses here performed the morphology of this species fell outside the variation of all the extant ecomorphogroups, thus suggesting the possibility that this species might have occupied a different niche in comparison to extant canids.

The role of phylogeny in the development of the frontal sinuses in Pleistocene fossil species of the genus *Canis*

The shape analyses performed in this paper and in previous papers (e.g., Curtis and Van Valkenburgh 2014; Frosali et al. 2023) highlighted the importance of ecology in determining the shape of frontal sinuses, but it is also undeniable that phylogeny plays a role in the development of this structure (i.e., frontal sinuses are considered a synapomorphy in the tribe Canini; Tedford et al. 1995, 2009). Despite its usefulness at higher taxonomic ranks, the PaCA suggests that sinus shape does not represent a very performant phylogenetic proxy when species are more closely related and possibly ecology plays a greater role. Nonetheless, we were able to extrapolate the polarity and direction of evolution of relevant morphological features, thus obtaining insights into the evolutionary history of frontal sinuses in the Canini tribe. Particularly, the stem Canini genus *Eucyon* diverged in a different evolutionary trajectory from the Canini total group LCA relative to all other Canini by the possession of a peculiar sinus morphology (i.e., a more rostrocaudal elongated sinus rather than medio-laterally enlarged one, with a slender rostrolateral lobe and an underdeveloped rostromedial one). Given the low covariation with phylogeny of the shape data, this might be the result of adaptation to different ecological preferences. Increasing the fossil dataset of this genus and better comprehending its actual phylogenetic position and relationship with other Caninae species might help clarify further the peculiar ecological adaptations of this stem Canini lineage and what the shape of the frontal sinus of the first stem Canini species actually was. It also must be noticed that the phylogenetic analysis is influenced by the chosen phylogeny, thus a possible change in the phylogenetic position of some species might influence possible future results. Similarly, the Cerdocyonina (except *Ch. brachyurus*, which retained the primitive morphology for the Canini) show a markedly different sinus morphology, which appears to have evolved away from the shape reconstructed for the crown Canini LCA. They differ from the subtribe Canina for the rostrocaudal shortened morphology of the sinus, with a medially divergent rostromedial lobe, a deeper rostral incision and the presence of a well-marked and defined caudal incision. The lack of a clear phylogenetic patterning within the subtribes at the species level (i.e., closely related species may show very distinct morphology) further suggests that differences in sinus morphology might be the result of adaptation to different ecological niches (e.g., *C. lupus* and *Canis latrans*). These results highlight that nuances in frontal sinus morphology are not useful for taxonomic affinity assessment at ranks below the subtribe, while the general morphology allows good discrimination at higher taxonomic level. This is exemplified by the case of similar evolutionary trajectories showed by *C. borjgali*, *C. etruscus* and *C. lupus*, which convergently diverged from the rest of the Canina.

Conclusions

The analyses performed in this work highlighted the value of the study of frontal sinuses to disentangle the diet and phylogeny of fossil canids. The results showed that both fossil and extant canid species possess a wide morphological variation in the frontal sinus. The plesiomorphic condition for sinus morphology is here reconstructed as being characterised by one rostrolateral lobe: from this basal plan different species in different clades have evolved, for ecological reasons, a second rostromedial lobe. As such, *Eucyon davisi*, the most basal of the two species of the genus *Eucyon* analysed, possesses only a rostrolateral lobe, while *E. adoxus*, a more derived species of this same genus, shows also a rostromedial lobe. Within Canini, both *Canis borjgali* and *Canis etruscus* present a sinus morphology characterised by one main rostrolateral lobe. They thus share a plesiomorphic sinus morphology, but many finer differences between these two species are also noticeable (e.g., *C. borjgali* shows

a more inflated and convoluted sinus and many dorsal and lateral sulci; Fig. 4a-b). Since nuances in sinus morphology seem more related to ecology rather than phylogeny, these differences underline the fact that these two different species probably occupied different ecological niches. Sinus shape analysis and the reconstructed paleodiet of *C. etruscus* both suggest a closer link with *Lu. adusta* than to the clade *Lycaon-Cuon-Canis*, suggesting that this fossil species had an ecological niche characterised by a high import of non-meat food in the diet (one of the specimens of *C. etruscus* is less clearly classified in the shape analyses, but the other one is mainly placed within the hypocarnivores variation). The main difference between *C. etruscus* and *Lu. adusta* is in their body mass, given the fact that *C. etruscus* is a much bigger species than *Lu. adusta*, but we see that it is possible to have a hypocarnivorous diet despite the large size (*Chrysocyon brachyurus* shows a body mass that is even bigger than that of *C. etruscus* and is classified as hypocarnivore). Instead, due to its more inflated and sulcated sinus morphology, *C. borjgali* is probably on the lineage of *Canis lupus*, together with *Canis mosbachensis* (as previous authors have suggested; Bartolini-Lucenti 2020; Sotnikova and Rook 2010): *C. lupus* indeed diverged from the last common ancestor with *Canis latrans* going in the same direction as *C. borjgali* (Fig. 10). Even if with strongly different morphologies, these two fossil species (i.e., *C. borjgali* and *C. mosbachensis*) possess more derived sinus structures in comparison to *C. etruscus* that places them close to the morphology of more carnivorous species. The peculiar morphology of *C. borjgali* did not fit well with the variation of all extant ecomorphogroups, possibly indicating that this species occupied a different ecological niche. *Canis mosbachensis* is instead consistent with the morphological variation observed in various extant species of the genus *Canis*, reinforcing once again the hypothesis that this species is strictly linked to the evolutionary line of this genus.

The understanding of evolutionary and ecological implications of the frontal sinus in canids is still at the beginning, but has already provided promising results, corroborating the feeding hypothesis as the main driver in shaping the morphology of this paranasal cavity also in the Caninae subfamily. The analyses performed here also start to shed light on the actual influence of phylogeny on the frontal sinus shape and structure. Hence, future research based on larger fossil canid samples will likely shed further light not only on the relevance of the frontal sinus in the ecology of this group, but will also help further clarify the debated phylogeny of this clade.

Supplementary Information The online version contains supplementary material available at https://doi.org/10.1007/s10914-026-09819-1.

Acknowledgements The authors are thankful to the kindness of the curators who allowed us to scan the specimens in their collections or to access them online: Paolo Agnelli, curator of the Zoological Museum “La Specola” (Museum of Natural History of the University of Florence, Italy); Andrea Savorelli, curator of the Geology and Paleontology Museum of Florence (University of Florence, Italy); Justin Adams, Senior Lecturer in the Centre for Human Anatomy Education, Department of Anatomy and Developmental Biology (Monash University in Clayton, Australia); Maia Bukhsianidze, David Lordkipanidze and Ann Margvelashvili of the Georgian National Museum. They are indebted to the staff of the San Giovanni di Dio Hospital (Florence, Italy), especially to Elisabetta Peruzzi and Giovanni Dedola and all the technicians of Medical Radiology ward (“SOS Radiologia”) for granting us access to their CT-scanner and support while processing raw data. The authors are grateful to Dr. Andrea Faggi (technical responsible of the “Paleo[Fab]Lab”, the Vertebrate Palaeontology Laboratory at the Earth Sciences Department of the University of Florence), for his care in specimen preparation, as well crucial support and advice on use and maintenance of laboratory equipments and instruments. The Paleo[Fab]Lab (Vertebrate Palaeontology Laboratory at the Earth Sciences Department of the University of Florence) is equipped with a set of advanced instrumentations acquired thanks to the Italian Ministry for Universities and Research (MIUR), “Departments of Excellence” funding (2023-2027), and the support of Project PE 0000020 CHANGES (CUP B53C22004010006, NRP Mission 4 Component 2 Investment 1.3) funded by the European Union – NextGenerationEU. S.B.L. thanks CERCA Programme/Generalitat de Catalunya.

Author contributions S.F. prepared the first draft of the manuscript. S.F., A.U. and S.B.L. revised and modified the manuscript reaching a definitive version. L.R. and J.M.M. reviewed and improved the manuscript definitive version. S.F. segmented the CT and microCT scans of the specimens to obtain the 3D models and performed the morphometric analysis. S.F. and A.U. performed the geometric morphometrics analyses. S.F. and S.B.L. prepared the figures. All authors read and agreed to the definitive version of the manuscript.

Funding Open access funding provided by Università degli Studi di Firenze within the CRUI-CARE Agreement.

Data availability All data generated and analyzed during this study are included in this published paper and its supplementary files. The CT and µCT scans used to recreate the 3D models of the frontal sinuses, and the 3D models themselves will be available through request to the corresponding author. The seven specimens of *C. aureus*, *C. lupus* and *Ch. brachyurus* (016_C_GDJK, 016_C2_GDJK, 016_C3_GDJK, 038_C_COY, 037_C_WOLF, 037_C2_WOLF, 147_C_MAWO) originally published by Czeibert et al. (2024) are available in the online repository FigShare (https://nc.elte.hu/s/doZnwPjgeBaZ7as).

Declarations

Competing interests The authors declare no competing interests.

Open Access This article is licensed under a Creative Commons Attribution 4.0 International License, which permits use, sharing, adaptation, distribution and reproduction in any medium or format, as long as you give appropriate credit to the original author(s) and the source, provide a link to the Creative Commons licence, and indicate if changes were made. The images or other third party material in this article are included in the article’s Creative Commons licence, unless indicated otherwise in a credit line to the material. If material is not included in the article’s Creative Commons licence and your intended

use is not permitted by statutory regulation or exceeds the permitted use, you will need to obtain permission directly from the copyright holder. To view a copy of this licence, visit http://creativecommons.org/licenses/by/4.0/.

References

Adams R, Cain Z, Assis R, DeGiorgio M (2024) Robust phylogenetic regression. Syst Biol 73:140–157. https://doi.org/10.1093/sysbio/syad070

Balzeau A, Albessard-Ball L, Kubicka AM, Filippo A, Beaudet A, Santos E, Bienvenu T, et al. (2022) Frontal sinuses and human evolution. Sci Adv 8(42):eabp9767. https://doi.org/10.1126/sciadv.abp9767

Bartolini-Lucenti S (2020) Evolutionary history of Canidae (Carnivora, Mammalia) and Lyncodontini (Mustelidae, Carnivora) in the Plio-Pleistocene of the Old World. Dissertation, Università di Pisa

Bartolini-Lucenti S, Rook L (2021) "*Canis*" *ferox* revisited: diet ecomorphology of some long gone (Late Miocene and Pliocene) fossil dogs. J Mamm Evol 28(2):285–306. https://doi.org/10.1007/s10914-020-09500-1

Bartolini-Lucenti S, Alba DM, Rook L, Moyà-Solà S, Madurell-Malapeira J (2017) Latest Early Pleistocene wolf-like canids from the Iberian Peninsula. Quat Sci Rev 162:12–25. https://doi.org/10.1016/j.quascirev.2017.02.023

Bartolini-Lucenti S, Bukhsianidze M, Martínez-Navarro B, Lordkipanidze D (2020) The wolf from Dmanisi and augmented reality: review, implications, and opportunities. Front Earth Sci 8:131. https://doi.org/10.3389/feart.2020.00131

Bartolini-Lucenti S, Madurell-Malapeira J, Martínez-Navarro B, Cirilli O, Pandolfi L, Rook L, Bushkhianidze M, et al. (2022) A comparative study of the Early Pleistocene carnivore guild from Dmanisi (Georgia). J Hum Evol 162:103108. https://doi.org/10.1016/j.jhevol.2021.103108

Blomberg SP, Garland T Jr, Ives AR (2003) Testing for phylogenetic signal in comparative data: behavioral traits are more labile. Evolution 57(4):717–745. https://doi.org/10.1111/j.0014-3820.2003.tb00285.x

Bône A, Louis M, Martin B, Durrleman S (2018) Deformetrica 4: An open-source software for statistical shape analysis. In: Reuter M, Wachinger C, Lombaert H, Paniagua B, Lüthi M, Egger B (eds) Shape in Medical Imaging. Springer International Publishing, Cham, pp 3–13

Brugal JP, Boudadi-Maligne M (2011) Quaternary small to large canids in Europe: taxonomic status and biochronological contribution. Quat Int 243(1):171–182. https://doi.org/10.1016/j.quaint.2011.01.046

Cardini A, Polly PD (2020) Cross-validated between group PCA scatterplots: a solution to spurious group separation? Evol Biol 47(1):85–95

Chavez DE, Gronau I, Hains T, Dikow RB, Frandsen PB, Figueiró HV, Garcez FS, et al. (2022) Comparative genomics uncovers the evolutionary history, demography, and molecular adaptations of South American canids. Proc Natl Acad Sci U S A 119(34):e2205986119. https://doi.org/10.1073/pnas.2205986119

Cherin M, Bertè DF, Sardella R, Rook L (2013) *Canis etruscus* (Canidae, Mammalia) and its role in the faunal assemblage from Pantalla (Perugia, central Italy): comparison with the Late Villafranchian large carnivore guild of Italy. Boll Soc Paleontol Ital 52:11–18. https://doi.org/10.4435/BSPI.2013.05

Cherin M, Bertè DF, Rook L, Sardella R (2014) Re-defining *Canis etruscus* (Canidae, Mammalia): a new look into the evolutionary history of early Pleistocene dogs resulting from the outstanding fossil record from Pantalla (Italy). J Mamm Evol 21(1):95–110. https://doi.org/10.1007/s10914-013-9227-4

Collyer ML, Adams DC (2021) Phylogenetically aligned component analysis. Methods Ecol Evol 12:359–372. https://doi.org/10.1111/2041-210X.13515

Curtis AA, Van Valkenburgh B (2014) Beyond the sniffer: frontal sinuses in Carnivora. Anat Rec 297(11):2047–2064. https://doi.org/10.1002/ar.23025

Czeibert K, Nagy G, Csörgő T, Donkó T, Petneházy Ö, Csóka Á, Garamszegi LZ, et al. (2024) High-resolution computed tomographic (HRCT) image series from 413 canid and 18 felid skulls. Sci Data 11(1):753. https://doi.org/10.1038/s41597-024-03572-x

Del Campana D (1913) Cani pliocenici della Toscana. Palaeon Ital 19:189–254

Durrleman S, Prastawa M, Charon N, Korenberg JR, Joshi S, Gerig G, Trouvé A (2014) Morphometry of anatomical shape complexes with dense deformations and sparse parameters. NeuroImage 101:35–49. https://doi.org/10.1016/j.neuroimage.2014.06.043

Engelman RK (2022) Occipital condyle width (OCW) is a highly accurate predictor of body mass in therian mammals. BMC Biol 20:37. https://doi.org/10.1186/s12915-021-01224-9

Evans HE, De Lahunta A, Miller ME (2013) Miller's Anatomy of the Dog. Elsevier Saunders, St. Louis

Fedorov A, Beichel R, Kalpathy-Cramer J, Finet J, Fillion-Robin J-C, Pujol S, Bauer C, et al. (2012) 3D Slicer as an image computing platform for the quantitative imaging network. Magn Reson Imaging 30(9):1323–1341. https://doi.org/10.1016/j.mri.2012.05.001

Felsenstein J (1985) Phylogenies and the comparative method. Am Nat 125(1):1–15. https://doi.org/10.1086/284325

Ferring R, Oms O, Agustí J, Berna F, Nioradze M, Shelia T, Tappen M, et al. (2011) Earliest human occupations at Dmanisi (Georgian Caucasus) dated to 1.85–1.78 Ma. Proc Natl Acad Sci U S A 108(26):10432–10436. https://doi.org/10.1073/pnas.1106638108

Fischer G (1817) Adversaria Zoologica. Mem Soc Imp Nat Mosc 5:357–472

Flower LOH, Schreve DC (2014) An investigation of palaeodietary variability in European Pleistocene canids. Quat Sci Rev 96:188–203. https://doi.org/10.1016/j.quascirev.2014.04.015

Forsyth Major CI (1877) Considerazioni sulla fauna dei mammiferi pliocenici e post-pliocenici della Toscana - III. Cani fossili del Val D'Arno superiore e della Valle d'Era. Mem Soc Tosc Sci Nat 3:207–227

Frisch JL (1775) Das Natur-System der Vierfüssigen Thiere, in Tabellen: Darinnen alle Ordnungen, Geschlechte und Arten, Nicht nur mit Bestimmenden Benennungen, Sondern Beygesetzten Unterscheidenden Kennzeichen Angezeigt Werden, zum Nutzen der Erwachsenen Schuljugend. Günther, Glogau

Friscia AR, Van Valkenburgh B, Biknevicius AR (2007) An ecomorphological analysis of extant small carnivorans. J Zool 272(1):82–100. https://doi.org/10.1111/j.1469-7998.2006.00246.x

Frosali S, Bartolini-Lucenti S, Madurell-Malapeira J, Urciuoli A, Costeur L, Rook L (2023) First digital study of the frontal sinus of stem-Canini (Canidae, Carnivora): evolutionary and ecological insights throughout advanced diagnostic in paleobiology. Front Ecol Evol 11:1173341. https://doi.org/10.3389/fevo.2023.1173341

Gray J (1821) On the natural arrangement of vertebrose animals. London Med Repos 15:296–310

Gray J (1834) Illustrations of Indian Zoology, Chiefly Selected from the Collection of Major-General Hardwicke. Volume 2. Treuttel, Wurz, Treuttel, Jun. and Richter, Paris

Harvey PH, Pagel MD (1991) The Comparative Method in Evolutionary Biology. Oxford University Press, Oxford

Hemprich WF, Ehrenberg CG (1830) Symbolae Physicae, Seu, Icones et Descriptiones, Icones et Descriptiones Mammalium quae ex Itinere per Africam Borealem et Asiam Occidentalem. Berolini, Ex Officina Academica

Hemprich WF, Ehrenberg CG (1833) Symbolae Physicae, Seu Icones et Descriptiones Corporum Naturalium Novorum aut Minus Cognitorum quae ex Itineribus per Libyam, Aegyptium, Nubiam, Dongalam, Syriam, Arabiam et Habessiniam. Pars Zool II. Berolini, Ex Officina Academica, Berlin

Huxley TH (1880) On the cranial and dental characters of the Canidæ. Proc Zool Soc Lond 48: 238–288. https://doi.org/10.1111/j.1469-7998.1880.tb06558.x

Illiger JCW (1811) Prodromus Systematis Mammalium et Avium: Additis Terminis Zoographicis Utriusque Classis, Eorumque Versione Germanica. Sumptibus C. Salfeld, Berlin, Germany

Iurino DA, Mecozzi B, Iannucci A, Moscarella A, Strani F, Bona F, Gaeta M, et al. (2022) A Middle Pleistocene wolf from central Italy provides insights on the first occurrence of *Canis lupus* in Europe. Sci Rep 12(1): 2882. https://doi.org/10.1038/s41598-022-06812-5

Joeckel RM (1998) Unique frontal sinuses in fossil and living Hyaenidae (Mammalia, Carnivora): description and interpretation. J Vertebr Paleontol 18:627–639. https://doi.org/10.1080/02724634.1998.10011089

Klecka WR (1980) Discriminant Analysis. SAGE Publications, Beverly Hills

Lindblad-Toh K, Wade CM, Mikkelsen TS, Karlsson EK, Jaffe DB, Kamal M, Clamp M, et al. (2005) Genome sequence, comparative analysis and haplotype structure of the domestic dog. Nature 438(7069):803–819. https://doi.org/10.1038/nature04338

Linnaeus C von (1758) Systema Naturae per Regna Tria Naturae secundum Classes, Ordines, Genera, Species, cum Characteribus, Differentiis, Synonymis, Locis., Editio Decima. Laurentii Salvii, Stockholm, Sweden

Linnaeus C von (1766) Systema naturae per Regna Tria Naturae secundum Classes, Ordines, Genera, Species, cum Characteribus, Differentiis, Synonymis, Locis, Editio Duodecima. Laurentii Salvii, Stockholm, Sweden

Martin R (1973) Trois nouvelles especes de Caninae (Canidae, Carnivora) des gisements plio-villafranchiens d'Europe. Doc Lab Géol Fac Sci Lyon 57:87–96

Martínez-Navarro B, Bartolini-Lucenti S, Palmqvist P, Ros-Montoya S, Madurell-Malapeira J, Espigares M-PPM-P (2021) A new species of dog from the Early Pleistocene site of Venta Micena (Orce, Baza Basin, Spain). C R Palevol 20:297–314. https://doi.org/10.5852/cr-palevol2021v20a17

McGreevy P, Grassi TD, Harman AM (2004) A strong correlation exists between the distribution of retinal ganglion cells and nose length in the dog. Brain Behav Evol 63:13–22. https://doi.org/10.1159/000073756

Meloro C (2011) Feeding habits of Plio-Pleistocene large carnivores as revealed by the mandibular geometry. J Vertebr Paleontol 31(2): 428–446. https://doi.org/10.1080/02724634.2011.550357

Merriam JC (1911) Tertiary mammal beds of Virgin Valley and Thousand Creek in north-western Nevada. Part II: Vertebrate faunas. Univ Cal Publ Geol 11:199–304

Mitteroecker P, Bookstein F (2011) Linear discrimination, ordination, and the visualization of selection gradients in modern morphometrics. Evol Biol 38:100–114. https://doi.org/10.1007/s11692-011-9109-8

Pagel MD (1999) Inferring the historical patterns of biological evolution. Nature 401(6756):877–884

Pallas PS (1811) Zoographia Rosso-Asiatica Sistens Omnium Animalium in Extenso Imperio Rossico et Adjacentibus Maribus Observatorum Recensionem, Domicilia, Mores et Descriptiones, Anatomen atque Icones Plurimorum. Volumen Secundum. Caes, Academiae Scientiarium Impress, Saint Petersburg

Palmqvist P, Arribas A, Martinez Navarro B (1999) Ecomorphological study of large canids from the lower Pleistocene of southeastern Spain. Lethaia 32:75–88

Pearse WD, Davies TJ, Wolkovich EM (2023) How to define, use, and interpret Pagel's λ (lambda) in ecology and evolution. Glob Ecol Biogeogr 34(4):e70012

Peri E, Bartolini-Lucenti S, Tseng ZJ, Rook L (2025) Biomechanical bite simulation in *Eucyon davisi* (Mammalia, Canidae) and comparison with extant canids. Sci Rep 15:25786. https://doi.org/10.1038/s41598-025-95939-2

Pérez-Ramos A, Figueirido B (2020) Toward an "ancient" virtual world: improvement methods on x-ray CT data processing and virtual reconstruction of fossil skulls. Front Earth Sci 8:345

Qiu Z, Deng T, Wang B (2004) Early Pleistocene mammalian fauna from Longdan, Dongxiang, Gansu, China. Palaeontol Sinica N Ser C 191:1–245

R Core Team (2024) R: A language and environment for statistical computing, Vienna, Austria

Revell LJ (2024) phytools 2.0: an updated R ecosystem for phylogenetic comparative methods (and other things). PeerJ 12:e16505. https://doi.org/10.7717/peerj.16505

Rook L (2009) The wide ranging genus *Eucyon* Tedford & Qiu, 1996 (Mammalia, Carnivora, Canidae, Canini) in the Mio-Pliocene of the Old World. Geodiversitas 31:723–741. https://doi.org/10.5252/g2009n4a723

Rook L, Torre D (1996) The wolf-event in western Europe and the beginning of the Late Villafranchian. Neu Jahr Geol Paläontol-Monat 8:495–501.

Rüppell E (1835) Neue Wirbelthiere zu der Fauna von Abyssinien Gehörig. S. Schmerber, Frankfurt am Main

Say T (1823) Account of an Expedition from Pittsburgh to the Rocky Mountains, Performed in the Years 1819 and '20, by Order of the Hon. J.C. Calhoun, Sec'y of War: under the Command of Major Stephen H. Long. From the Notes of Major Long, Mr. T. Say, and Other Gentlemen of the Exploring Party. H.C. Carey and I. Lea, Philadelphia

Schlager S (2017) Morpho and Rvcg – shape analysis in R. In: Zheng G, Li S, Szekely G (eds) Statistical Shape and Deformation Analysis: Methods Implementations and Applications. Elsevier, London, pp 217–256

Schreber JCD (1775) Die Säugthiere in Abbildungen Nach der Natur mit Beschreibungen. W. Walther, Erlangen

Sclater PL (1883) The Secretary read the following reports on the additions made to the Society's Menagerie during the months of June, July, August, September, and October, 1882. Proc Sci Meet Zool Soc Lond 1882:631

Soergel W (1925) Die säugetierfauna des altdiluvialen Tonlagers von Jockgrim in der Pfalz. Z Deutsch Geol Ges 77:405–438

Sotnikova M, Rook L (2010) Dispersal of the Canini (Mammalia, Canidae: Caninae) across Eurasia during the Late Miocene to Early Pleistocene. Quat Int 212:86–97. https://doi.org/10.1016/j.quaint.2009.06.008

Sundevall CJ (1846) Nya mammalia från Sydafrika. Öfvers Kongl Vetensk-Akad Förh 3:118–123

Tedford RH, Qiu Z (1996) A new canid genus from the Pliocene of Yushe, Shanxi Province. Vertebr PalAsiat 34:27–40

Tedford RH, Wang X (2008) *Metalopex*, a new genus of fox (Carnivora: Canidae: Vulpini) from the late Miocene of western North America In: Wang X, Barnes LG (eds) Geology and Vertebrate Paleontology of Western and Southern North America. Contributions in Honor of David P. Whistler. Nat Hist Mus Los Angel Co Sci Ser No. 41:273–278

Tedford RH, Taylor BE, Wang X (1995) Phylogeny of the Caninae (Carnivora: Canidae): the living taxa. Am Mus Novit 3146:1

Tedford RH, Wang X, Taylor BE (2009) Phylogenetic systematics of the North American fossil Caninae (Carnivora: Canidae). Bull Am Mus Nat Hist 2009(325):1–218. https://doi.org/10.1206/574.1

Teilhard de Chardin P (1940) The fossils from Locality 18 near Peking. Palaeontol Sin N Ser C 9:1–94

Temminck (1820) Annales Générales des Sciences Physiques. L'Imprimerie de Weissenbruch, Bruxelles

Torre D (1967) I cani villafranchiani della Toscana. Palaeont Ital 53:113–138

Tseng ZJ, Wang X (2010) Cranial functional morphology of fossil dogs and adaptation for durophagy in *Borophagus* and *Epicyon* (Carnivora, Mammalia). J Morphol 271:1386–1398. https://doi.org/10.1002/jmor.10881

Turner A (1995) The Villafranchian large carnivore guild: geographic distribution and structural evolution. Alp Mediterr Quat 8:349–356

Urciuoli A, Zanolli C, Beaudet A, Dumoncel J, Santos F, Moyà-Solà S, Alba DM (2020) The evolution of the vestibular apparatus in apes and humans. eLife 9:e51261. https://doi.org/10.7554/eLife.51261

Van Valkenburgh B (1989) Carnivore dental adaptations and diet: A study of trophic diversity within guilds. In: Gittleman JL (ed) Carnivore Behavior, Ecology and Evolution. Volume 1. Springer, Berlin, pp 410–436

Van Valkenburgh B (2007) Déjà vu: The evolution of feeding morphologies in the Carnivora. Integr Comp Biol 47:147–163. https://doi.org/10.1093/icb/icm016

Van Valkenburgh B, Koepfli K-P (1993) Cranial and dental adaptations to predation in canids. Symp Zool Soc Lond 65:15–37

Van Valkenburgh B, Sacco T, Wang X (2003) Pack hunting in Miocene borophagine dogs: evidence from craniodental morphology and body size. Bull Am Mus Nat Hist 279:147–162

Vinuesa V (2018) Bone-cracking hyenas (Carnivora, Hyaenidae) from the European Neogene and Quaternary: taxonomy, paleobiology and evolution. Dissertation, Universitat Autonoma de Barcelona

Vinuesa V, Madurell-Malapeira J, Fortuny J, Alba DM (2015) The endocranial morphology of the Plio-Pleistocene bone-cracking hyena *Pliocrocuta perrieri*: behavioral implications. J Mamm Evol 22(3):421–434. https://doi.org/10.1007/s10914-015-9287-8

Vinuesa V, Iurino DA, Madurell-Malapeira J, Liu J, Fortuny J, Sardella R, Alba DM (2016) Inferences of social behavior in bone-cracking hyaenids (Carnivora, Hyaenidae) based on digital paleoneurological techniques: implications for human–carnivoran interactions in the Pleistocene. Quat Int 413:7–14. https://doi.org/10.1016/j.quaint.2015.10.037

Wang X, Tedford RH, Antón M (2008) Dogs: Their Fossil Relatives and Evolutionary History. Columbia University Press, New York

Zanolli C, Kaifu Y, Pan L, Xing S, Mijares AS, Kullmer O, Schrenk F, et al. (2022) Further analyses of the structural organization of *Homo luzonensis* teeth: evolutionary implications. J Hum Evol 163:103124. https://doi.org/10.1016/j.jhevol.2021.103124

Zrzavý J, Řičánková V (2004) Phylogeny of recent Canidae (Mammalia, Carnivora): relative reliability and utility of morphological and molecular datasets. Zool Scr 33:311–333. https://doi.org/10.1111/j.0300-3256.2004.00152.x

Publisher's note Springer Nature remains neutral with regard to jurisdictional claims in published maps and institutional affiliations.